^{103}Pd/^{103m}Rh – Comments on evaluation of decay data

by A. L. Nichols[1], T. Kibédi[2]

[1] Department of Physics, University of Surrey, Guildford GU2 7XH, UK
[2] Department of Nuclear Physics, The Australian National University (ANU), Canberra ACT, Australia

Reviewer: S. Leblond

Université Paris-Saclay, CEA, Laboratoire National Henri Becquerel (LNE-LNHB), 91120 Palaiseau, France

Evaluated: March/April 2021, September/October 2021, October 2023, June 2024

Evaluation Procedures

Limitation of Relative Statistical Weight Method (LWM) and other analytical techniques were applied to average numbers throughout the evaluation. The uncertainty assigned to the average value was always greater than or equal to the smallest uncertainty of the values used to calculate the average.

Decay Scheme

^{103}Pd ($T_{½}$ = 17.00 days) decays almost 100% by electron capture decay (Q_{EC} = 534.9 (24) keV) to the metastable excited state of ^{103m}Rh to be followed by IT decay ($T_{½}$ = 56.115 minutes) to the ground state of ^{103}Rh (Q_{IT} = 39.753 (6) keV), as quantified in 2021Wa16 and 2021Ko07. While the full EC decay process consists of four EC transitions and nine gamma-ray emissions to the ground state of ^{103}Rh, the decay scheme is dominated by EC decay directly to the 39.753-keV excited state of ^{103m}Rh and the resulting IT gamma transition to the stable ^{103}Rh ground state. However, a number of difficulties arise as a consequence of the lack of significant agreement between the X-ray and gamma-ray measurements of 1969Zo02, 1969Gr13, 1970NiZV, 1976Ma37, 2002Bf07, 2004Po24, 2018Ri01 and 2021Ri01 (particularly the important relative emission probability of the 39.753-keV gamma ray). Under these rather difficult circumstances, the decision was taken to assess the weighted-mean relative emission probabilities of the gamma-ray studies by 1976Ma37 and 2021Ri01 on the basis of their reported accuracy, consistency and completeness, along with consideration of data subsets selected from the measurements of 1969Zo02, 2002Bf07 and 2004Po24. All relative gamma-ray emission probabilities were defined in terms of the 357.42-keV gamma ray (100).

Nuclear Data

There is a strong interest in the well-defined nuclear levels of ^{103}Rh populated in the EC decay of ^{103}Pd because of the adoption of this monoisotopic element (^{103}Rh) as a neutron flux monitor. ^{103}Pd decay is also viewed as a suitable electron and X-ray emitter for microdosimetry and radiotherapy in nuclear medicine.

Half-life of ^{103}Pd

The measurements of 1953Me24, 1975Cz05, 1981Va11 and 2021Ri01were adopted to give a weighted mean half-life of 17.00 (5) days based on the LWM analytical technique (Avetools code, version 3.0, and V.AveLib 06-22 code, both ENSDF utility programs).

Reference	Half-life (d)	Selected detail, issues and uncertainties
1947Ma32	17.0	no uncertainty quoted – not adopted in analytical procedures
1948Li03	17	no uncertainty quoted – not adopted in analytical procedures
1953Me24	**17.0 ± 0.4**	long-lived component after neutron irradiation of Pd target (Geiger-Muller tube: activity followed over 60 d)
1954Ri09	17.5 ± 0.5	X rays, total γ spectrum, 60- to 250-, 367- and 503-keV γ rays (NaI(Tl) crystal over 15 d (reference Fig. 2)); outlier (Chauvenet criterion) – not adopted in analytical procedures
1968Pa24	16.9 ± 0.1	sparse information - analysis of X-ray decay curves from proton-irradiated silver and indium targets (NaI(Tl) crystal over unspecified times) – not adopted in analytical procedures
1969Gr13	18.4 ± 0.5	conversion/Auger electrons, KX rays and γ rays (double-focussing β spectrometer and Ge(Li) detector over 70 d); significant outlier (Chauvenet criterion) – not adopted in analytical procedures
1975Cz05	**16.961 ± 0.016[a]**	conversion/Auger electrons (4π-proportional flow counter over 80 d) and 20-keV KX rays (NaI(Tl) crystal and Ge(Li) detector over 32 and 36 d, respectively) – focus on Ge(Li) data
1981Va11	**16.991 ± 0.019[b]**	decay of KX rays (Si(Li) detectors) and γ rays (NaI(Tl) crystal over 33 to 54 d); detailed definition of systematic uncertainties
2004Po24	16.8 ± 0.6	decay of 295-, 358- and 479-keV γ rays over ~ 100 d by means of HPGe detector; outlier – not adopted in final analytical procedure
2021Ri01	**17.049 ± 0.016**	regular determination of peak area of 357.4-keV γ ray over 50 d by means of HPGe detector; well-defined uncertainties
Recommended value	**17.00 ± 0.05**	**LWM, with uncertainty expanded from ± 0.03 to ± 0.05 to cover 17.049 ± 0.016 of 2021Ri01; χ^2/(N-1) of 5.18 and $\chi^2/(N-1)_{critical}$ at 99% confidence level of 3.78 after a second pass; UWM of 17.000 ± 0.018**

[a] Weighted mean of three sets of measurements is 16.953 (7), compared with an adopted value of 16.961 (16) quoted by 1975Cz05.
[b] Weighted mean of four sets of measurements is 16.992 (10), compared with an adopted value of 16.991 (19) quoted by 1981Va11.

Consideration was given to the unweighted mean (UWM), limitation of relative statistical weight method (LWM), normalised residual method (NRM), Rajeval technique, expected value method (EVM), bootstrap method and Mandel-Paule approach in analyses of the data set.

Analytical method	Half-life (d)	χ^2/(N-1)	χ^2/(N-1)$_{critical}$
UWM	17.00 ± 0.10	–	–
LWM	17.00 ± 0.03	5.18	2.60 for rejection at 95% confidence level
NRM	16.984 ± 0.017	2.19	2.60 for rejection at 95% confidence level
Rajeval	16.990 ± 0.016	0.69	2.60 for rejection at 95% confidence level
EVM	17.00 ± 0.08	–	89.3% confidence level
Bootstrap	17.00 ± 0.06	5.19	–
Mandel-Paule	17.001 ± 0.033	5.18	–

Although a number of difficulties arose during the course of this exercise, a half-life value of (17.00 ± 0.05) days was derived and recommended for ^{103}Pd, as quantified by the LWM analytical procedure. However, these studies demonstrated the requirement for further accurate measurements of this decay parameter.

Half-life of daughter ^{103m}Rh

The measurements of 1967VuZZ, 1969KoZW, 1973Gu06, 1974Sa15, 1978La21 and 1981Va11 were adopted to give a weighted mean half-life of 56.115 (16) min based on the LWM-NRM-Rajeval analytical techniques.

Reference	Half-life (min)	Selected detail, issues and uncertainties
1944Fl01	48 ± 5	^{103}Rh(n$_f$,n') reaction – outlier (Chauvenet criterion), and therefore not included in analytical procedures
1945Wi03/1945Wi12	45 ± 1	^{103}Rh(X,γ) reaction – outlier (Chauvenet criterion), and therefore not included in analytical procedures
1947Fl03	52 ± 2	^{103}Rh(d,d') reaction – outlier (Chauvenet criterion), and therefore not included in analytical procedures
1950Me26	56	separation of Pd target and ^{103m}Rh – uncertainty not specified, and therefore not included in analytical procedures
1957Jo19	57.5 ± 0.5	^{103}Rh(n,n') reaction – outlier (Chauvenet criterion), and therefore not included in analytical procedures
1967VuZZ	**56.6 ± 0.4**	^{103}Rh(n,n') reaction; 4π proportional counter and thin NaI crystal
1969KoZW	**56.6 ± 0.6**	^{102}Ru(n,γ)^{103}Ru(β$^-$)^{103m}Rh; radiochemical separation, NaI(Tl) scintillation counter
1972Pa10	57.5	^{103}Rh(n$_{14.7keV}$,n') reaction, Si(Li) detector – uncertainty not specified, and therefore not included in analytical procedures
1973Gu06	**56.116 ± 0.009**	^{nat}Pd(n,xn')^{103}Pd(EC)^{103m}Rh; three counting techniques: liquid scintillation counter, 2π-methane flow counter, and NaI(Tl) crystal – weighted mean of three sets of measurements is 56.116 (7), compared with a value of 56.116 (9) quoted by 1973Gu06; uncertainty adjusted to ± 0.016 to reduce weighting to ~ 0.50
1974Sa15	**56.3 ± 0.6**	^{103}Rh(n,n') reaction; decay curve followed over many half-lives, NaI(Tl) X-ray detector
1978La21	**56.112 ± 0.028**	ion exchange of ^{103m}Rh from ^{103}Pd solutions; decay curves involving 15 sources followed over three half-lives by means of an ill-defined photon spectrometer
1979VaZE	56.1 ± 0.1	preliminary measurement - replaced by half-life determined by 1981Va11
1981Va11	**56.114 ± 0.020**	ion exchange of ^{103m}Rh from ^{103}Pd solutions; decay curves followed over two and three half-lives, NaI(Tl) detector – weighted mean of two sets of measurements is 56.114 (12), compared with a value of 56.114 (20) quoted by 1981Va11
Recommended value	**56.115 ± 0.016**	recommended uncertainty adjusted from ± 0.011 to ± 0.016, to align with smallest uncertainty of the values used to calculate weighted-mean value

Limitation of relative statistical weight method (LWM), normalized residual method (NRM), Rajeval technique, expected value method (EVM), bootstrap method and Mandel-Paule approach were considered in the analysis of the data set.

Analytical method	Half-life (min)	χ^2/(N-1)	χ^2/(N-1)$_{critical}$
UWM	56.31 ± 0.16	–	–
LWM	56.115 ± 0.011	0.45	2.21 for rejection of 95.0% confidence level
NRM	56.115 ± 0.011	0.45	2.21 for rejection at 95.0% confidence level
Rajeval	56.115 ± 0.011	0.45	2.21 for rejection at 95.0% confidence level
EVM	56.13 ± 0.08	–	97.0% confidence level
Bootstrap	56.22 ± 0.16	15.8	–
Mandel-Paule	56.115 ± 0.011	0.45	–

Half-life of (56.115 ± 0.016) minutes was recommended for ^{103m}Rh, as quantified by the LWM-NRM analytical procedures (with 1973Gu06 uncertainty increased to ± 0.016 in order to adjust weighting to ~ 0.50).

^{103}Pd/^{103m}Rh parent-daughter equilibrium

Q values

A Q_{EC} value for ^{103}Pd EC decay of 534.9 (24) keV to the excited metastable state of ^{103m}Rh and subsequent

IT decay with Q_{IT} of 39.753 (6) keV to the ground state of ^{103}Rh have been adopted (2021Ko07, 2021Wa16), to give a Q_{EC} value of 574.7 (24) keV for ^{103}Pd EC decay to the stable ground state of ^{103}Rh.

Gamma-ray energies and emission probabilities

Energies

The energies of the gamma-ray emissions have been reasonably well measured by 1969Zo02, 1969Gr13, 1969Ra18, 1970NiZV, 1970Pe04, 1976Ma37 and 2010Kr05, and therefore individual weighted-mean values were determined from these data. GTOL version 7.2h (24-May-2013) is an ENSDF analysis code that was used to undertake least-squares fits to the evaluated gamma-ray energies, and re-define the energies of the proposed nuclear levels of ^{103}Rh for comparison with the equivalent level energies recommended by 2009De29. Nuclear-level energies were subsequently determined in this manner, except for the highly-converted (E3 + M4) 39.753-keV gamma transition and associated nuclear level which were preferably identified with a gamma transition energy of 39.7537 (21) keV as determined from K_{ce} and the K-shell electron binding energy (2000KoZT), and also in exact alignment with a Q_{IT} of 39.753 (6) keV adopted in NUBASE2020 (2021Ko07, 2021Wa16).

Adopted energies, spins and parities for the nuclear levels of ^{103}Rh (GTOL v7.2h and 2009De29).

Nuclear level number	Nuclear level energy (keV)		Spin and parity	Half-life
	GTOL v7.2h	2009De29		
0	0.0	0.0	1/2 $^-$	stable
1	39.752 ± 0.006	**39.753 ± 0.006**	7/2 $^+$	(56.115 ± 0.016) min.
2	**93.034 ± 0.008**	93.036 ± 0.009	9/2 $^+$	(1.11 ± 0.03) ns [a]
3	**294.965 ± 0.010**	294.965 ± 0.008	3/2 $^-$	
4	**357.40 ± 0.03**	357.396 ± 0.017	5/2 $^-$	
5	**536.839 ± 0.008**	536.840 ± 0.007	5/2 $^+$	

[a] Weighted-mean value of 1.114 (24) ns determined from measurements of 1.13 (3) ns by plastic scintillator and 1.13 (7) ns by beta spectrometer (1972Ja01) and 1.06 (5) ns by delayed coincidence with NaI(Tl) detector and plastic scintillator (1973Ba52); uncertainty increased from ± 0.024 to ± 0.03 ns in alignment with the smallest uncertainty of the values used to calculate the weighted mean.

Emission Probabilities

Relative gamma-ray emission probabilities have been partially or fully determined in the measurements of 1969Zo02, 1969Gr13, 1970NiZV, 1976Ma37, 2002Bf07, 2004Po24 and 2021Ri01 by means of various numbers/arrays and types of high-resolution Ge(Li) detector and HPGe (significantly earlier studies of 1954Ri09, 1955Av11 and 1955Sa16 involved the use of NaI(Tl) scintillators). Unfortunately, specific subsets of the more recent individual datasets are judged as being disparate – relative gamma-ray emission probabilities normalised to P_γ(357.38 keV) of 100 differ widely by a factor of 1.2 to 2.0 for the prominent 39.753- and 62.41-keV gamma-ray emissions as measured by 1976Ma37 and 2021Ri01 when compared with the equivalent measurements of 1969Zo02 and 1970NiZV, while more modest disagreement is found to within a factor of between 0.7 to 0.8 for the higher-energy 62.4-, 295- and 497-keV gamma rays. There are also similar modest disagreements between 1976Ma37/2021Ri01 and 1969Gr13 for the 62.4-, 295- and 497-keV gamma rays, although the relative gamma-ray emission probability of the dominant 39.753-keV gamma ray as measured by 1969Gr13 is a significant factor of 2.6/2.2 smaller than that determined by 1976Ma37/2021Ri01. Under these rather difficult circumstances, the decision was taken to favour overall the measurements of Macias *et al*. (1976Ma37) and Riffaud *et al.* (2021Ri01) on the basis of their reported accuracy, consistency and completeness.

The experimental studies of Macias *et al*. involved the thermal-neutron irradiation of palladium enriched to 93% ^{102}Pd. Gamma spectra were studied by means of 20- and 40-cm^3 Ge(Li) detectors with energy resolutions FWHM ≤ 2.2 keV for 1332-keV gamma rays. A planar 0.5-cm^3 Ge(Li) crystal was used to quantify low-energy photon spectra, while an anti-Compton spectrometer consisting of an 8-cm^3 Ge(Li) diode and NaI(Tl) annulus was also employed in the gamma spectral studies. A commercial solution of ^{103}Pd was acquired by 2021Ri01 for subsequent dilution and the preparation of six sources suitable for gamma-ray spectroscopic studies. N-type HPGe detectors were used to determine the gamma-ray emission probabilities: two 100 cm^3 coaxial detectors were used over the energy range 50 to 500 keV, while KX-ray and low-energy gamma-ray emissions were measured by means of a planar detector along with LX-ray studies undertaken with an additional silicon drift detector. Despite the perceived thoroughness of these two particular set of measurements by 1976Ma37 and 2021Ri01, further extensive gamma- and X-ray studies are required to improve future efforts to derive a comprehensive decay scheme with any great confidence beyond quantification of the dominant EC decay to the 39.753-keV excited state of ^{103m}Rh and the resulting IT gamma transition to the stable ground state of ^{103}Rh.

Directly measured and recommended gamma-ray energies.

E_γ (keV)											
1954Ri09 ^{103}Pd(EC)	**1955Av11 ^{103}Pd(EC)**	**1955Sa16 ^{103}Ru(β⁻) ^{103}Pd(EC)**	**1969Zo02 ^{103}Ru(β⁻) ^{103}Pd(EC)**	**1969Gr13 ^{103}Pd(EC)**	**1969Ra18 ^{103}Ru(β⁻)**	**1970NiZV ^{103}Ru(β⁻) ^{103}Pd(EC)**	**1970Pe04 ^{103}Ru(β⁻)**	**1976Ma37 ^{103}Ru(β⁻) ^{103}Pd(EC)**	**2010Kr05 ^{103}Ru(β⁻)**	**2018Ni14 2009ENSDF**	**Weighted mean (LWM)[a]**
–	40.0 (5)[b]	40	**39.78 (5)**	**39.748 (8)**	**39.755 (12)**	**39.75 (7)**	**39.762 (16)**	**39.73 (2)**	–	–	**39.750 ± 0.006 → 39.753 ± 0.006[c,d]**
–	53?	–	**53.28 (5)**	–	**53.275 (10)**	**53.3 (9)**	**53.271 (30)**	**53.29 (1)**	**53.286 (10)**	53.282 (7)	**53.283 ± 0.006**
–	65 (1)	65 (3)	**62.3 (2)**	**62.30 (12)**	–	**62.5 (1)**	–	**62.41 (3)**	–	–	**62.41 ± 0.03**
262 (15)	–	–	**241.8 (1)**	262?	–	–	**241.87 (25)**	**241.88 (5)**	**241.875 (10)**	–	**241.875 ± 0.010**
305 (8)	298 (2)	300 (5)	**295.17 (10)**	**294.70 (17)**	**294.72 (12)**	**295.0 (1)**	**294.82 (8)**	**294.98 (15)**	**294.964 (10)**	294.964 (10)[e]	**294.962 ± 0.015**
	~ 330	–	**318.0 (3)**	330?	–	**317.4 (3)**	–	**317.72 (5)**	–	–	**317.72 ± 0.05**
367 (6)	362 (3)	365 (5)	**357.60 (10)**	**356.98 (9)**	–	**357.5 (1)**	**357.21 (35)**	**357.45 (8)**	**357.382 (23)**	–	**357.38 ± 0.08**
–	–	–	444.11 (15)[b]	–	**443.77 (12)**	**443.9 (1)**	**443.63 (12)**	**443.79 (5)**	**443.810 (10)**	443.80 (2)	**443.809 ± 0.010**
503 (8)	498 (4)	495 (5)	**497.23 (10)**	496.74 (22)[b]	**497.080 (13)**	**497.1 (1)**	**496.92 (10)**	**497.08 (2)**	**497.085 (10)**	497.083 (6)	**497.083 ± 0.007**

[a] Weighted mean of selected gamma-ray energy measurements (no adjustments made to the weighting of the input uncertainties to give both the LWM values and uncertainties listed).
[b] Chauvenet outlier, and therefore not included in final AveTools analytical procedures to determine LWM.
[c] Single gamma transition of IT decay of ^{103m}Rh daughter.
[d] Recommended E_γ of 39.753 (6) keV in close agreement with ^{103m}Rh gamma transition energy of 39.7537 (21) keV determined from K_{ce} and K electron binding energy by Kovalík *et al*. (2000KoZT), and aligned exactly with Q_{IT} of 39.753 (6) keV as adopted in NUBASE2020/AME2020 (2021Ko07, 2021Wa16).
[e] A value of 295.964 (10) keV was erroneously listed in Table III of 2018Ni14 – acknowledged within a direct communication from the lead author, and therefore corrected to 294.964 (10) keV (2009De29).

Published gamma-ray emission probabilities.

E_γ (keV)	P_γ					
	1954Ri09[b]	**1955Av11[c]**	**1955Sa16[b]**	**1969Zo02[d]**	**1969Gr13[b]**	**1970NiZV[e]**
39.753 ± 0.006[a]	−	0.0021 (2)	~ 0.1	211 (10)	0.072 (6)	1100 (90)[g]
53.283 ± 0.006	−	≤ 0.000005[h]	−	0.03 (1)	−	0.23
62.41 ± 0.03	−	0.000040 (6)	0.004 (1)	2.4 (2)	0.0042 (4)	20 (3)
241.875 ± 0.010	0.004 (2)[h]	−	−	−	< 0.0005[h]	−
294.962 ± 0.015	} 0.011 (3)	0.00030 (3)	0.012 (2)	14.2 (14)	0.0108 (14)	72 (8)
317.72 ± 0.05		~ 0.0001	−	0.04 (1)	< 0.0005[h]	0.41 (8)
357.38 ± 0.08	0.060 (7)	0.0021 (4)	0.066 (10)	100.0	0.0610 (30)	531 (5)
443.809 ± 0.010	−	−	−	0.075 (8)	−	0.23 (6)
497.083 ± 0.007	0.011 (2)	0.00045 (5)	0.01	17.5 (18)	0.0140 (14)	100 (10)

Published gamma-ray emission probabilities (continued).

E_γ (keV)	P_γ			
	1976Ma37[f]	**2002Bf07[d]**	**2004Po24[d]**	**2021Ri01[b]**
39.753 ± 0.006[a]	100	−	–	0.0647 (7)
53.283 ± 0.006	0.038 (30)	−	–	< 0.000008
62.41 ± 0.03	1.52 (5)	−	–	0.001128 (16)
241.875 ± 0.010	0.0007 (7)[h]	−	−	–
294.962 ± 0.015	4.1 (1)	14.08 (35)	12.3 (2)	0.00315 (7)
317.72 ± 0.05	0.022 (1)	−	–	0.0000137 (17)
357.38 ± 0.08	32.3 (10)	100.0 (19)	100.0 (10)	0.02486 (17)
443.809 ± 0.010	0.022 (1)	−	−	0.000021 (8)
497.083 ± 0.007	5.8 (2)	18.15 (36)	17.6 (3)	0.00439 (7)

[a] Single gamma transition of ^{103m}Rh daughter (IT decay).
[b] Expressed as absolute gamma-ray emission probabilities per decay (1954Ri09, 1955Sa16, 1969Gr13 - factor of 10 adjustment made to reported data of 1954Ri09), and per 100 decays (2021Ri01).
[c] Emission probabilities expressed relative to total P_{XK} of 1.0.
[d] Emission probabilities expressed relative to Pγ(357.38 keV) of 100.0.
[e] Emission probabilities expressed relative to Pγ(497.81 keV) of 100 (10).
[f] Emission probabilities expressed relative to Pγ(39.753 keV) of 100.
[g] Statistical uncertainty only.
[h] Gamma emission not observed with confidence.

Measured and recommended gamma-ray emission probabilities relative to P_γ(357.42 keV) of 100.

E_γ (keV)	P_γ^{rel}					
	1954Ri09[a]	**1955Av11[a]**	**1955Sa16[a]**	**1969Zo02**	**1969Gr13[a]**	**1970NiZV[a]**
39.753 ± 0.006[c]	–	100 (21)	~ 150	211 (10)	118 (12)	207 (17)[d]
53.283 ± 0.006	–	≤ 0.24	–	0.03 (1)	–	0.04
62.41 ± 0.03	–	1.9 (5)	6 (2)	2.4 (2)	6.9 (7)	3.8 (6)
241.875 ± 0.010	7 (4)	–	–	–	< 0.8	–
294.962 ± 0.015	18 (6)	14 (3)	18 (4)	14.2 (14)	17.7 (25)	13.6 (15)
317.72 ± 0.05		~ 5	–	0.04 (1)	< 0.8	0.077 (15)
357.38 ± 0.08	100 (16)	100 (30)	100 (21)	100.0	100 (7)	100 (1)
443.809 ± 0.010	–	–	–	**0.075 (8)**	–	0.043 (11)
497.083 ± 0.007	18 (4)	21 (5)	15	**17.5 (18)**	23 (3)	18.8 (19)

Measured and recommended gamma-ray emission probabilities relative to P_γ(357.42 keV) of 100 (continued).

E_γ (keV)	P_γ^{rel}				
	1976Ma37[a]	**2002Bf07**	**2004Po24**	**2021Ri01[a]**	**Recommended[b]**
39.753 ± 0.006[c]	310 (10)	–	–	**260 (3)**	**260 (3)[e]**
53.283 ± 0.006	0.12 (9)	–	–	< 0.032	**0.0231 (13)[f]**
62.41 ± 0.03	**4.71 (21)**	–	–	**4.54 (7)**	**4.56 (7)**
241.875 ± 0.010	0.0022 (22)	–	–	–	**0.0032(3)[g]**
294.962 ± 0.015	**12.7 (5)**	14.08 (35)	**12.3 (2)**	**12.7 (3)**	**12.5 (2)[h]**
317.72 ± 0.05	**0.068 (4)**	–	–	**0.055 (7)**	**0.065 (6)**
357.38 ± 0.08	**100 (4)**	**100.0 (19)**	**100.0 (10)**	**100.0 (7)**	**100.0**
443.809 ± 0.010	**0.068 (4)**	–	–	**0.08 (3)**	**0.070 (4)**
497.083 ± 0.007	**18.0 (8)**	**18.15 (36) → 18.2 (4)**	**17.6 (3)**	**17.7 (3)**	**17.8 (3)[i]**

[a] Emission probabilities adjusted in order to be expressed relative to P_γ(357.38 keV) of 100 or 100.0.
[b] Apart from the highly-converted 39.753-keV γ ray and low-intensity 53.283- and 241.875-keV γ rays, weighted-mean values of the measured relative emission probabilities were adopted with uncertainties that do not fall below the most precise measurement, unless stated otherwise in the footnotes below.
[c] Single γ emission in the IT decay of daughter ^{103m}Rh.
[d] Statistical uncertainty only.
[e] While the relative transition probability of the 39.753-keV γ ray is extremely important in defining the decay scheme with any degree of confidence, measurements of this parameter over many years have proved to be difficult and significantly disparate – a value of 260 (3) has been adopted on the basis of the recent well-defined measurement by 2021Ri01.
[f] A relative emission probability of 0.0231 (13) was adopted to achieve γ population-depopulation balance and a direct β^- population of zero for the 93.034-keV nuclear level of ^{103}Rh.
[g] Gamma emission not observed with confidence in the EC decay of ^{103}Pd – tentative value of 0.0032 (3) adopted for P_γ^{rel}(241.875 keV) from equivalent studies of ^{103}Ru β^- decay of 0.0029 (3) (1976Ma37) and 0.0035 (3) (1994Sc43) involving relevant γ decays from the 536.839-kev nuclear level of ^{103}Rh.
[h] LWM value of 12.45 (16) adjusted to 12.5 (2) to avoid the uncertainty falling below the most precise measurement.
[i] LWM value of 17.78 (18) adjusted to 17.8 (3) to avoid the uncertainty falling below the most precise measurement.

While a high fraction of the decay of ^{103}Pd is identified with direct EC population of the 39.753-keV nuclear level of ^{103m}Rh, a number of other higher-energy levels are also populated and undergo subsequent gamma depopulation. However, there is little to no agreement between the various sets of gamma-ray measurements that strive to quantify the lesser EC and gamma transitions. Weighted-mean analyses of the relative emission probabilities for those gamma rays with energies below 290 keV were only performed with data from 1976Ma37 and 2021Ri01, while other supportive data were taken from 1969Zo02, 2002Bf07 and 2004Po24 for gamma-ray energies above 290 keV. This whole approach can only be described as questionable, and emphasizes the need for further gamma-ray measurements.

Another feature of note is that the ^{103m}Rh IT decay (half-life of 56.115 minutes) via a single gamma transition to the ground state of ^{103}Rh has been included in this evaluation of the ^{103}Pd decay scheme, with an appropriate adjustment of the emission probability of the 39.753-keV gamma ray.

Multipolarities, and Internal Conversion Coefficients

A significant number of studies have focussed on the measurement and derivation of internal conversion coefficients and mixing ratios, particularly with respect to the ^{103m}Rh IT transition of 39.753 keV. Relevant measured and proposed data have been collected together in a series of tables displayed below, along with other related parameters such as ICC shell and subshell ratios.

Gamma-ray emissions: proposed mixing ratios of (M1 + E2) gamma transitions.

E_γ (keV)	δ				
	1977Kr13 recommended	**1981Ha11** Measured	**1981Mu18** measured	**1983Kr01** re-determined	**Recommended**
53.28	0.000 (55)	–	–	–	0.00 (5)
294.96	– 0.17 (1)[a]	–	–	–	– 0.170 (13)
497.08	– 0.125 (10)	**– 0.36 (8)**[a,b]	**– 0.42 (4)**[a]	**– 0.368 (11)**[a]	– 0.371 (35)

[a] Used in BrIccMixing calculations to determine the recommend mixing ratio.
[b] Preferred δ value of – 0.36 (8) from gamma-ray angular distributions measurements of β^- decay of ^{103}Ru ground state ($3/2^+$) at temperatures down to 2.8 mK, compared with δ value of – 0.34 (5) for β^- decay of ^{103}Ru ground state ($5/2^+$).

The multipolarities of the gamma transitions have been defined on the basis of the known spins and parities of the relevant nuclear levels of ^{103}Rh (2009De29), coupled with various determinations of the ICCs and subshell ratios:

39.753-keV isomeric transition of ^{103m}Rh defined as (99.935%E3 + 0.065%M4) from a wide range of ICC and subshell ratio measurements (particularly α_K and α_L of 2018Ni14) in support of a small M4 admixture from which a mixing ratio of 0.025 (+10, –15) was adopted;

53.283-keV gamma transition assumed to be virtually 100%M1 from the ICC data of 1970Pe04 and 1976Ma37;

62.41-keV gamma transition judged to be 100%M1 from α_L determination by 1969Gr13 of 0.13 (4) compared with a frozen orbital approximation of 0.14;

241.875-keV gamma transition defined as pure E1 from spin and parity considerations ($5/2^+ \rightarrow 3/2^-$), and supported by α_K measurements of 1970Pe04 and 1976Ma37;

294.962-keV gamma transition calculated to be 97.2%M1 + 2.8%E2 from recommended δ-value of – 0.170 (13) – see also 1958Mc02, 1970RoZS, 1972Sa03 and 1977Kr13 – as supported by α_K measurements of 1969Gr13, 1969Ra18, 1970Pe04 and 1976Ma37;

317.72-keV gamma transition defined as pure E1 from spin and parity considerations ($5/2^- \rightarrow 7/2^+$);

357.38-keV gamma transition defined as pure E2 from spin and parity considerations ($5/2^- \rightarrow 1/2^-$), and supported by α_K measurements of 1969Gr13 and 1976Ma37;

443.809-keV gamma transition assumed to be pure E2 from α_K measurements of 1970Pe04, 1971Av03 and 1976Ma37, and spin parity considerations ($5/2^+ \rightarrow 9/2^+$);

497.083-keV gamma transition calculated to be 87.9%M1 + 12.1%E2 from recommended δ-value of – 0.371 (35) – see 1981Ha11, 1981Mu18 and 1983Kr01 – as supported by α_K , α_L and subshell ratios determined by 1952Co16, 1968Ma08, 1969Zo02, 1970Pe04, 1970NiZV, 1971Av03 and 1976Ma37.

Recommended internal conversion coefficients have been determined by means of the BrIcc code (frozen orbital approximation) of Kibédi *et al*. (2008Ki07), based on the theoretical model of Band *et al*. (2002Ba85, 2002Ra45).

Gamma-ray emissions: measured and derived internal conversion coefficients, shell and subshell ratios, and mixing ratios.

E_γ (keV)		1950Ko10	1952Co16	1955Av11	1955Dr43	1955Mc51	1958Mc02	1967Br04	1967VuZZ	1968Ma08	1969Gr13[a]	1969Le17
39.753, E3 + M4	α_K	–	–	40	–	–	–	–	–	–	(145)	180 (20)
	α_L	–	–	470	–	–	–	–	–	1280 (260)	–	–
	α_M	–	–	–	–	–	–	–	–	–	–	–
	α_{total}	–	–	–	–	–	–	–	–	–	–	–
	α_K / α_{total}	–	–	–	–	–	–	–	–	–	–	–
	δ	–	–	–	–	–	–	–	–	–	–	–
	K/(K+L+M)	–	–	–	–	–	–	–	0.099 (10)[c]	–	–	–
	K/L	–	0.10 (4)[c]	0.09 (1)	0.18 (3)	–	–	–	–	–	–	–
	K/(L+M)	0.20 (4)	–	–	–	–	–	–	–	–	–	–
	K/(L+M+N)	–	–	–	–	–	–	0.0986 (50)	–	–	–	–
	K/(L+M+N+ …...)	–	–	–	–	–	–	–	–	–	–	–
	K/L_1	–	–	–	–	–	–	–	–	–	17 (6)	–
	K/L_2	–	–	–	–	–	–	–	–	–	0.357 (30)[c]	–
	K/L_3	–	–	–	–	–	–	–	–	–	0.243 (20)[c]	–
	K/ΣL	–	–	–	–	–	–	–	–	–	0.143 (12)[c]	–
	L_1/L_2	–	–	–	–	–	–	–	–	–	0.021 (6)	–
	L_1/L_3	–	–	–	–	–	–	–	–	–	0.013 (4)	–
	L_2/L_3	–	–	–	–	–	–	–	–	–	0.682 (11)[c]	–
	$M_{1,2}/M_3$	–	–	–	–	–	–	–	–	–	–	–
	$M_{1-3}/M_{4,5}$	–	–	–	–	–	–	–	–	–	33 (14)	–
	$M_{4,5}/M_3$	–	–	–	–	–	–	–	–	–	–	–
	M_3/L_3	–	–	–	–	–	–	–	–	–	–	–
	ΣL/ΣM	–	–	–	7 (1)	–	–	–	–	4.8 (7)[c]	4.90 (13)[c,e]	–
	N/M_3	–	–	–	–	–	–	–	–	–	–	–
	NO/M_3	–	–	–	–	–	–	–	–	–	–	–
	NO/M	–	–	–	–	–	–	–	–	–	–	–
	ΣL/ΣN	–	–	–	–	–	–	–	–	–	34 (3)[c]	–
53.283, (M1)	α_K	–	–	–	–	–	–	–	–	–	–	–
	α_L	–	–	–	–	–	–	–	–	–	–	–
	K/L	–	–	–	–	–	–	–	–	8.5 (9)	–	–
	L_1/L_2	–	–	–	–	–	–	–	–	–	–	–
	L_1/L_3	–	–	–	–	–	–	–	–	–	–	–
	L_2/L_3	–	–	–	–	–	–	–	–	–	–	–
62.41, M1 + E2	α_L	–	–	–	–	–	–	–	–	–	0.13 (4)[c]	–
241.875, E1	α_K	–	–	–	–	–	–	–	–	–	–	–
294.962, M1 + E2	α_K	–	–	–	–	–	–	–	–	0.024 (4)	0.017 (8)[c]	–
	δ	–	–	–	–	- 0.18 or - 1.17	- 0.17 (1)[c] or - 1.2	–	–	–	–	–
357.38, E2	α_K	–	–	–	–	–	–	–	–	–	0.0121 (21)[c]	–
443.809, E2	α_K	–	–	–	–	–	–	–	–	0.012 (2)	–	–
497.083, M1 + E2	α_K	–	–	–	0.0054 (10)	–	–	–	–	0.007 (1)	0.0029 (22)	–
	α_L	–	–	–	–	–	–	–	–	–	–	–
	K/L	–	8.5 (15)[c]	–	6.0 (15)	–	–	–	–	8.5 (7)[c]	–	–
	K/(L+M+ ……)	–	–	–	–	–	–	–	–	–	–	–
	$L_1/(L_2 + L_3)$	–	–	–	–	–	–	–	–	–	–	–
	δ	–	–	–	–	–	–	–	–	–	–	–

Gamma-ray emissions: measured and derived internal conversion coefficients, shell and subshell ratios, and mixing ratios (continued).

E_γ (keV)		1969Ra18	1969Zo02	1970NiZV	1970Pe04	1970RoZS	1971Av03	1972Br02	1972Pa10	1972Sa03	1974CzZY, 1975Cz03
39.753, E3 + M4	α_K	–	–	138 (5)[c]	159 (25)	–	–	–	123 (14)[c]	–	127 (6)[c]
	α_L	–	–	–	–	–	–	–	–	–	–
	α_M	–	–	–	–	–	–	–	–	–	–
	α_{total}	–	–	–	–	–	–	–	–	–	1531 (30)[c]
	α_K / α_{total}	–	–	–	–	–	–	–	–	–	0.0826 (50)
	δ	–	–	–	–	–	–	–	–	–	–
	K/(K+L+M)	–	–	–	–	–	–	–	–	–	–
	K/L	–	–	–	–	–	–	–	–	–	–
	K/(L+M)	–	–	–	–	–	–	–	–	–	–
	K/(L+M+N)	–	–	–	–	–	–	–	–	–	–
	K/(L+M+N+ .....)	–	–	–	–	–	–	–	–	–	0.0914 (43)
	K/L_1	–	–	–	–	–	–	–	–	–	–
	K/L_2	–	–	–	–	–	–	–	–	–	–
	K/L_3	–	–	–	–	–	–	–	–	–	–
	K/ΣL	–	–	–	–	–	–	–	–	–	–
	L_1/L_2	–	–	–	0.023 (4)[c]	–	–	–	–	–	–
	L_1/L_3	–	–	–	0.0163 (25)	–	–	0.00922 (208)	–	–	–
	L_2/L_3	–	–	–	0.695 (6)[c]	–	–	0.710 (15)[c]	–	–	–
	$M_{1,2}/M_3$	–	–	–	–	–	–	–	–	–	–
	$M_{1-3}/M_{4,5}$	–	–	–	–	–	–	–	–	–	–
	$M_{4,5}/M_3$	–	–	–	–	–	–	–	–	–	–
	M_3/L_3	–	–	–	–	–	–	–	–	–	–
	ΣL/ΣM	–	–	–	–	–	–	–	–	–	–
	N/M_3	–	–	–	–	–	–	–	–	–	–
	NO/M_3	–	–	–	–	–	–	–	–	–	–
	NO/M	–	–	–	–	–	–	–	–	–	–
	ΣL/ΣN	–	–	–	–	–	–	–	–	–	–
53.283, (M1)	α_K	–	–	1.77 (3)	1.90 (19)[c]	–	2.47 (14)	–	–	–	–
	α_L	–	–	–	–	–	–	–	–	–	–
	K/L	–	–	–	–	–	–	–	–	–	–
	L_1/L_2	–	–	–	12.1 (35)	–	–	–	–	–	–
	L_1/L_3	–	–	–	41 (20)[c]	–	–	–	–	–	–
	L_2/L_3	–	–	–	3.4 (20)[c]	–	–	–	–	–	–
62.41, M1 + E2	α_L	–	–	–	–	–	–	–	–	–	–
241.875, E1	α_K	–	–	–	0.013 (5)[c]	–	–	–	–	–	–
294.962, M1 + E2	α_K	0.016 (5)[c]	–	0.020 (5)	0.0176 (17)[c]	–	–	–	–	–	–
	δ	–	–	–	–	– 0.189 (10)[c]	–	–	–	0.15 (1)[c]	–
357.38, E2	α_K	–	–	–	> 0.011	–	–	–	–	–	–
443.809, E2	α_K	0.012 (3)	–	0.011 (3)	0.0062 (7)[c]	–	0.0064 (27)[c]	–	–	–	–
497.083, M1 + E2	α_K	0.0058 (15)	0.0043 (6)[c]	0.005 (1)[c]	(0.00459)	–	0.0044 (4)[c]	–	–	–	–
	α_L	–	–	–	–	–	–	–	–	–	–
	K/L	–	–	–	8.40 (25)[c]	–	–	–	–	–	–
	K/(L+M+ ……)	–	–	–	–	–	8.4 (4)	–	–	–	–
	$L_1/(L_2 + L_3)$	–	–	–	18.5 (35)	–	–	–	–	–	–
	δ	–	–	–	–	–	–	–	–	–	–

Gamma-ray emissions: measured and derived internal conversion coefficients, shell and subshell ratios, and mixing ratios (continued).

E_γ (keV)		1975Ma32[b]	1976Ma37	1977Kr13	1979VaZE	1981Ha11	1981Mu18	1983Kr01	1999Sa78	2018Ni14
39.753,	α_K	–	137 (19)[c]	–	148 (18)	–	–	–	153 (6)	141.1 (23)[c]
E3 + M4	α_L	–	1014 (11)	–	–	–	–	–	1185 (59)	–
	α_M	–	–	–	–	–	–	–	234 (15)	–
	α_{total}	–	–	–	1430 (89)[c]	–	–	–	–	1428 (13)[c]
	α_K / α_{total}	–	–	–	–	–	–	–	–	–
	δ	–	–	–	–	–	–	–	–	0.023 (5)[c]
	K/(K+L+M)	–	–	–	–	–	–	–	–	–
	K/L	–	–	–	–	–	–	–	–	–
	K/(L+M)	–	–	–	–	–	–	–	–	–
	K/(L+M+N)	–	–	–	–	–	–	–	–	–
	K/(L+M+N+ ……)	–	–	–	–	–	–	–	–	–
	K/L_1	–	–	–	–	–	–	–	–	–
	K/L_2	–	–	–	–	–	–	–	–	–
	K/L_3	–	–	–	–	–	–	–	–	–
	K/ΣL	–	–	–	–	–	–	–	–	–
	L_1/L_2	0.063 (12)[d]	–	–	–	–	–	–	–	–
	L_1/L_3	0.0432 (13)[d]	–	–	–	–	–	–	–	–
	L_2/L_3	0.684 (21)[c]	–	–	–	–	–	–	–	–
	$M_{1,2}/M_3$	0.76 (4)[c]	–	–	–	–	–	–	–	–
	$M_{1-3}/M_{4,5}$	–	–	–	–	–	–	–	–	–
	$M_{4,5}/M_3$	0.045 (9)[c]	–	–	–	–	–	–	–	–
	M_3/L_3	0.215 (9)[c]	–	–	–	–	–	–	–	–
	ΣL/ΣM	–	–	–	–	–	–	–	–	–
	N/M_3	0.259 (10)[c]	–	–	–	–	–	–	–	–
	NO/M_3	0.274 (15)[c]	–	–	–	–	–	–	–	–
	NO/M	0.150 (8)[c]	–	–	–	–	–	–	–	–
	ΣL/ΣN	–	–	–	–	–	–	–	–	–
53.283,	α_K	–	2.02 (10) and 1.74 (17) → av. 1.95 (13)[c]	–	–	–	–	–	–	–
(M1)	α_L	–	0.18 (2)[c]	–	–	–	–	–	–	–
	K/L	–	–	–	–	–	–	–	–	–
	L_1/L_2	–	–	–	–	–	–	–	–	–
	L_1/L_3	–	–	–	–	–	–	–	–	–
	L_2/L_3	–	–	–	–	–	–	–	–	–
62.41,	α_L	–	–	–	–	–	–	–	–	–
M1 + E2										
241.875, E1	α_K	–	0.011 (3)[c]	–	–	–	–	–	–	–
294.962,	α_K	–	0.018 (2)[c]	–	–	–	–	–	–	–
M1 + E2	δ	–	–	– 0.17 (1)[c]	–	–	–	–	–	–
357.38, E2	α_K	–	0.019 (11)[c]	–	–	–	–	–	–	–
443.809, E2	α_K	–	0.0069 (7)[c]	–	–	–	–	–	–	–
497.083,	α_K	–	0.0046 (1)[c]	–	–	–	–	–	–	–
M1 + E2	α_L	–	0.00055 (3)[c]	–	–	–	–	–	–	–
	K/L	–	8.4 (5)[c]	–	–	–	–	–	–	–
	K/(L+M+ ……)	–	–	–	–	–	–	–	–	–
	$L_1/(L_2 + L_3)$	–	–	–	–	–	–	–	–	–
	δ	–	–	– 0.125 (10)	–	– 0.36 (8)[c]	– 0.42 (4)[c]	– 0.368 (11)[c]	–	–

Above table - footnotes:

[a] Theoretical α_K value of 145 was adopted from 1968Ha52 by the authors (1969Gr13), and all other related data were normalised with respect to this particular value.

[b] Published data are experimental/theoretical ratios of the defined conversion-electron intensities – these data have been converted into their definitive experimental shell and subshell ratios in order to compare with other known measurements.

[c] Used in BrIccMixing code calculations to support recommend mixing ratios for the 39.753-, 53.283-, 294.962- and 497.083-keV gamma transitions.

[d] Doubtful value arises from the very weak ill-defined L_1 line.

[e] Value of 4.90 (13) calculated from the measured L and M conversion-electron intensities differs from the value of 4.39 (13) tabulated by 1969Gr13.

Gamma multipolarities, and theoretical internal-conversion coefficients as calculated by the BrIcc code (frozen orbital approximation).

E_γ (keV)	Multipolarity	α_K	α_L	α_{L1}	α_{L2}	α_{L3}	α_M	α_N	α_O	α_{total}
39.753 (6)	99.935%E3 + 0.065%M4 $\delta = 0.025\ ^{+10}_{-15}$ (1950Ko10, 1952Co16, 1955Av11, 1955Dr43, 1967Br04, 1967VuZZ, 1968Ma08, 1969Gr13, 1969Le17, 1970NiZV, 1970Pe04, 1972Br02, 1972Pa10, 1975Cz03, 1975Ma32, 1976Ma37, 1979VaZE, 1999Sa78, 2018Ni14)	142 (7)	1051 (30)	13 (5)	423 (6)	615 (18)	214 (6)	31.4 (9)	0.024 (11)	1440 (40)
53.283 (6)	(M1) (1968Ma08, 1970NiZV, 1970Pe04, 1971Av03, 1976Ma37)	1.81 (3)	0.223 (4)	0.204 (3)	0.01407 (20)	0.00418 (6)	0.0415 (6)	0.00686 (10)	0.000338 (5)	2.08 (3)
62.41 (3)	M1 (1969Gr13)	1.143 (16)	0.1406 (20)	0.1294 (19)	0.00865 (13)	0.00258 (4)	0.0262 (4)	0.00433 (6)	0.000214 (3)	1.314 (19)
241.875 (10)	E1 (1970Pe04, 1976Ma37)	0.01033 (15)	0.001202 (17)	0.001078 (15)	0.0000504 (7)	0.0000734 (11)	0.000222 (4)	0.0000366 (6)	0.000001761 (25)	0.01179 (17)
294.962 (15)	97.2%M1 + 2.8%E2 $\delta = -0.170$ (13) (1955Mc51, 1958Mc02, 1968Ma08,1969Gr13, 1969Ra18, 1970NiZV, 1970Pe04, 1970RoZS, 1972Sa03, 1976Ma37, 1977Kr13)	0.01669 (24)	0.00199 (3)	0.00187 (3)	0.0000868 (20)	0.0000357 (18)	0.000370 (6)	0.0000613 (9)	0.00000308 (5)	0.0191 (3)
317.72 (5)	E1	0.00493 (7)	0.000571 (8)	0.000521 (8)	0.0000201 (3)	0.0000294 (5)	0.0001055 (15)	0.00001741 (25)	0.000000853 (12)	0.00563 (8)
357.38 (8)	E2 (1969Gr13, 1970Pe04, 1976Ma37)	0.01368 (20)	0.00181 (3)	0.001434 (21)	0.000195 (3)	0.0001768 (25)	0.000337 (5)	0.0000548 (8)	0.00000234 (4)	0.01588 (23)
443.809 (10)	E2 (1968Ma08, 1969Ra18, 1970NiZV, 1970Pe04, 1971Av03, 1976Ma37)	0.00698 (10)	0.000889 (13)	0.000742 (11)	0.0000790 (11)	0.0000677 (10)	0.0001655 (24)	0.0000270 (4)	0.000001215 (17)	0.00807 (12)
497.083 (7)	87.9%M1 + 12.1%E2 $\delta = -0.371$ (35) (1952Co16, 1955Dr43, 1968Ma08, 1969Gr13, 1969Ra18, 1969Zo02, 1970NiZV, 1970Pe04, 1971Av03, 1976Ma37, 1977Kr13, 1981Ha11, 1981Mu18, 1983Kr01)	0.00458 (7)	0.000539 (8)	0.000509 (8)	0.0000203 (8)	0.0000100 (8)	0.0001001 (15)	0.00001660 (24)	0.000000839 (12)	0.00524 (8)

Parent ^{103}Pd (half-life of 17.00 (5) d) in secular equilibrium with daughter ^{103m}Rh (half-life of 56.115 (16) min)

^{103m}Rh($t_{1/2}$) < ^{103}Pd($t_{1/2}$) → ^{103}Pd concentration /^{103m}Rh concentration = $\frac{c_{103Pd}\,(\lambda_{103mRh} - \lambda_{103Pd})}{c_{103mRh} \cdot \lambda_{103mRh}}$

at equal detection coefficients $(c_{103Pd} = c_{103mRh})$, i.e., identical gamma-ray emission energies:

^{103}Pd activity/^{103m}Rh activity = $\frac{(\lambda_{103mRh} - \lambda_{103Pd})}{\lambda_{103mRh}} = \frac{103Pd(t_{1/2}) - 103mRh(t_{1/2})}{103Pd(t_{1/2})}$

^{103m}Rh activity/^{103}Pd activity = $\frac{103Pd(t_{1/2})}{103Pd(t_{1/2}) - 103mRh(t_{1/2})} = \frac{17.00(5)}{17.00(5) - 0.038969(11)} = 1.0023\ (29)$

Normalisation factor – gamma rays and EC decay

EC decay directly to the ground state of ^{103}Rh was assumed to be effectively zero on the basis of spin and parity changes that would result in a first forbidden unique transition ($5/2^+ \rightarrow 1/2^-$ (2, yes)). Therefore, the normalisation factor (*NF*) of the relative γ-ray emission probabilities can be determined on the basis of direct γ population of the ground state of ^{103}Rh summing to 100%.

$\sum(absolute\ \gamma\ transition\ probabilities\ direct\ to\ ^{103}Rh\ ground\ state) = 100$

$\Sigma[\{P^{rel}_{slow\gamma}(39.753\ keV)\ x\ (1+\alpha_{tot})\} + \{P^{rel}_{\gamma}(294.962\ keV)\ x\ (1+\alpha_{tot})\} + \{P^{rel}_{\gamma}(357.38\ keV)\ x\ (1+\alpha_{tot})\}]\ x\ NF = 100$

$[(374660\ (11263)/1.0023\ (29)) + 12.74\ (20) + 101.588\ (23)]\ x\ NF = 100$

in which the secular equilibrium of parent ^{103}Pd and daughter ^{103m}Rh is recognised in terms of the delayed emission of the 39.753-keV γ ray (by a factor of 1.0023 (29))

373914 (11290) x *NF* = 100

NF = 100 / 373915 (11290) = 0.000267 ± 0.000008

An equivalent total EC summation calculation gives an identical value: NF = 0.000267 ± 0.000008

A normalisation factor of (0.000267 ± 0.000008) was adopted in order to determine the absolute transition and emission probabilities of the EC and γ rays from their relative values.

Transition and emission probabilities of 39.753-keV gamma ray derived from the precise decay scheme

Consider the EC and gamma population of the first excited state of ^{103}Rh:

$TP^{rel}_{\gamma}(39.753\ keV) = \Sigma[\{P^{abs}_{EC(0,1)} \div NF\} + \{TP^{rel}_{\gamma}(53.28\ keV)\} + \{TP^{rel}_{\gamma}(317.72\ keV)\} + \{TP^{rel}_{\gamma}(497.98\ keV)\}]$

= Σ[{99.9646 (9) ÷ 0.000267 (8)} + 0.071 (4) + 0.065 (6) + 17.9 (3)] = [374399 (11218) + 18.0 (3)] = 374417 (11218)

$TP^{abs}_{\gamma}(39.753\ keV)$ = 374417 (11218) x 0.000267 (8) = 100 (4)% from above,

and 99.9695 (12)%, if overall accuracy is aligned with the determination of $P^{abs}_{EC(0,1)}(534.9\ keV)$;
also adjustments to $P^{rel}_{\gamma}(39.753\ keV)$ = 260 (11) → 260 (3),
and $P^{abs}_{\gamma}(39.753\ keV)$ = 0.069375 (1926)% → 0.0694 (19)%.

Recommended gamma-ray energies, and relative and absolute emission probabilities and transition probabilities of 100% EC decay of ^{103}Pd/^{103m}Rh.

	E_γ (keV)	P^{rel}_{γ}	TP^{rel}_{γ}	P^{abs}_{γ} (%)[a]	Absolute transition probability (%)
$\gamma_{1,0}$	39.753 (6)	260 (3)	374417 (11218)	0.069375 (1926) → 0.0694 (19)[a]	100 (4) → 99.9695 (12)[b]
$\gamma_{2,1}$	53.283 (6)	0.0231 (13)	0.071 (4)	0.0000062 (4)	0.0000190 (12)
$\gamma_{4,3}$	62.41 (3)	4.56 (7)	10.55 (18)	0.00122 (4)	0.00282 (10)
$\gamma_{5,3}$	241.875 (10)	0.0032 (3)	0.0032 (3)	0.00000085 (8)	0.00000086 (8)
$\gamma_{3,0}$	294.962 (15)	12.5 (2)	12.74 (20)	0.00334 (11)[a]	0.00340 (11)
$\gamma_{4,1}$	317.72 (5)	0.065 (6)	0.065 (6)	0.0000174 (17)	0.0000175 (17)
$\gamma_{4,0}$	357.38 (8)	100.0	101.588 (23)	0.0267 (8)[a]	0.0271 (8)
$\gamma_{5,2}$	443.809 (10)	0.070 (4)	0.071 (4)	0.0000187 (12)	0.0000189 (12)
$\gamma_{5,1}$	497.083 (7)	17.8 (3)	17.9 (3)	0.00475 (16)	0.00477 (16)

[a] Uncertainties of P^{abs}_{γ} for three γ emissions that populate the ground state directly and sum to 100% in terms of their transition probabilities were assessed by means of the GABS code, version 12, 20 June 2021 to avoid double accounting of uncertainties (39.753-, 294.96- and 357.38-keV) → $P^{abs}_{\gamma}(39.753\ keV)$ re-defined as 0.0694 (19)% rather than 0.069 (22)%, whereas there is no equivalent impact on the uncertainties of P^{abs}_{γ}(294.96- and 357.38-keV).

[b] TP^{abs}_{γ} adjusted from 100 (4) on the basis of summed total TP_γ ground-state population of 100%, with contributions of 0.00340 (11)% and 0.0271 (8)% from the 294.96- and 357.38-keV γ transitions, respectively, to give a very precise TP_γ(39.753 keV) of 99.9695 (12)%.

The GABS code was used to convert the evaluated relative γ-ray emission probabilities to absolute values per 100 decays of the ^{103}Pd parent nucleus, along with their uncertainties (GABS, version 12, 20 June 2021,

ENSDF analysis program). Gamma rays that directly populate the nuclear levels involved in the calculation of the normalisation factor were identified prior to these calculations in order to avoid double accounting of their uncertainties during the course of this process.

Electron energies were determined from electron binding energies tabulated by Larkins (1977La19) and the evaluated gamma-ray energies. Absolute electron emission probabilities were calculated from the evaluated absolute gamma-ray emission probabilities and associated internal conversion coefficients.

Energies and emission probabilities of noteworthy internal conversion electrons from 100% EC decay of ^{103}Pd/^{103m}Rh.

		Energy (keV)	Electrons per 100 disint.
$ec_{1,0\ T}$	(Rh)	16.533 – 39.751	99.9695 (12)
$ec_{1,0\ K}$	(Rh)	16.533 (6)	9.9 (6)
$ec_{1,0\ L}$	(Rh)	36.341 – 36.749	73 (3)
$ec_{1,0\ M}$	(Rh)	39.126 – 39.446	14.9 (6)
$ec_{1,0\ N+}$	(Rh)	39.672 – 39.751	2.2 (1)

The relatively simple decay scheme of ^{103}Pd is completely dominated by the EC transition which populates the 39.753-keV metastable state of ^{103}Rh with an absolute EC transition probability of 99.9646%. As a consequence, all other gamma transitions possess low to extremely low absolute transition probabilities, apart from the 39.753-keV gamma decay from ^{103m}Rh to the stable ground state of ^{103}Rh. Under such circumstances, there is also no evidence of reasonable agreement between the seven sets of experimental studies in which Ge(Li) detectors of good resolution were used to measure the gamma-ray emission probabilities (1969Zo02, 1969Gr13, 1970NiZV, 1976Ma37, 2002Bf07, 2004Po24 and 2021Ri01). Despite some misgivings, the more extensive measurements of 1976Ma37 and 2021Ri01 were most regularly accepted in this evaluation along with other more limited γ-ray emission data to be found within 1969Zo02, 2002Bf07 and 2004Po24. Furthermore, a relative P_γ(53.283 keV) of 0.0231 (13) was calculated by achieving a balanced gamma population-depopulation of the 93.031-keV nuclear level of ^{103}Rh, while a tentative value of 0.0032 (3) was adopted for the relative P_γ(241.85 keV) on the basis of equivalent β^- decay studies of ^{103}Ru (1976Ma37, 1994Sc43). Although the assumption that no EC transition populates the ^{103}Rh ground state directly is questionable, the transition probability has been judged to be sufficiently low as to assign a value of zero, while direct EC decay to the 93.031-keV nuclear level of ^{103}Rh was similarly defined as zero from spin-parity considerations.

EC Transitions

Energies

The recommended nuclear level energies and evaluated Q_{EC}-value of 574.7 (24) keV for the ^{103}Pd ground-state to ^{103}Rh ground-state transition were used to determine the recommended energies and uncertainties of the EC transitions (2021Wa16).

Transition Probabilities

EC transition probabilities were derived for the population-depopulation imbalances of the relative emission probabilities of the gamma rays and their theoretical internal-conversion, and a normalisation factor of 0.000267 ± 0.000008 for the gamma-ray emissions as calculated above. EC decay directly to both the 93.031-keV nuclear level and ground state of ^{103}Rh were assumed to be effectively zero on the basis of spin and parity considerations that would result in second forbidden non-unique and first forbidden unique transitions, respectively. The BetaShape code was adopted to calculate the log*ft* and fractional EC probabilities P_K, P_L, P_M and P_N, as defined and developed further from the data tabulations of 1995ScZY and 1998Sc28 (BetaShape code, version 2.3.1, December 2023, LNHB analysis program (2015Mo10, 2019Mo35, 2023Mo21)).

Recommended EC decay of ^{103}Pd as derived by means of the BetaShape code (2015Mo10, 2019Mo35, 2023Mo21).

	E_{EC} (keV)[a]	P_{EC} (%)	^{103}Pd	^{103}Rh	transition type	log *ft*	P_K	P_L	P_{L1}	P_{L2}
$EC_{0,5}$	37.9 (24)	0.00480 (16)	5/2 +	5/2 +	allowed	7.33 (11)	0.55 (5)	0.35 (4)	0.34 (4)	0.0065 (7)
$EC_{0,4}$	217.3 (24)	0.0300 (9)	5/2 +	5/2 −	first forbidden non-unique	8.569 (18)	0.8459 (6)	0.1226 (4)	0.1204 (4)	0.002255 (8)
$EC_{0,3}$	279.7 (24)	0.00058 (7)	5/2 +	3/2 −	first forbidden non-unique	10.52 (5)	0.8518 (5)	0.11804 (26)	0.11587 (25)	0.002171 (6)
$EC_{0,2}$	481.7 (24)	zero	5/2 +	9/2 +	[second forbidden non-unique]	–	–	–	–	–
$EC_{0,1}$	534.9 (24)	99.9646 (9)	5/2 +	7/2 +	allowed	5.880 (6)	0.86086 (30)	0.11103 (15)	0.10899 (15)	0.002047 (4)
$EC_{0,0}$	574.7 (24)	zero	5/2 +	1/2 −	[first forbidden unique]	–	–	–	–	–
		Σ 100.0000 (13)								

[a] Determined from the recommended nuclear level energies and Q-value of 574.7 (24) keV (2021Wa16).

	E_{EC} (keV)[a]	P_M	P_N
$EC_{0,5}$	37.9 (24)	0.084 (11)	0.0186 (25)
$EC_{0,4}$	217.3 (24)	0.02589 (17)	0.00563 (6)
$EC_{0,3}$	279.7 (24)	0.02479 (14)	0.00538 (5)
$EC_{0,2}$	481.7 (24)	–	–
$EC_{0,1}$	534.9 (24)	0.02310 (11)	0.00501 (4)
$EC_{0,0}$	574.7 (24)	–	–

A consistent decay scheme was derived that consists of four EC transitions and nine gamma-ray emissions (with the 39.753-keV gamma decay of ^{103m}Rh included in the existing data set), of which almost all of the EC decay is directly to the 39.753-keV metastable state of ^{103}Rh ((99.9646 ± 0.0009)%).

Atomic Data

Measurements of the total KX-ray emission probability and Auger-electron emission probabilities have been carried out, and are listed below for ^{103}Ru as well as ^{103}Pd and ^{103m}Rh. The X-ray related data of direct applicability to the ^{103}Pd-^{103m}Rh system has been assessed more thoroughly in terms of the measurements of P_{KX}, $P_{K\alpha}/P_{K\beta}$ and P_γ(357.42 keV)/P_{KX}. As listed in the table below, the experimental studies of the KX emission probabilities associated with ^{103}Pd EC decay exhibit reasonable agreement (1976Ma37, 1978Ne09, 2002Bf07, 2021Ri01), and compare well with the BrIccEmis/NS_RadList calculation for $P_{KXtotal}$ of 77.5%. Furthermore, the measured KX emission probabilities for the 39.753-keV gamma transition of ^{103m}Rh are in good agreement (1967Br04, 1967VuZZ, 1969Gr13, 1973In07, 1974Sa15, 1975Cz03, 1981Va22, 1994Sc43, 2018Ri01), and are well aligned with the BrIccEmis/NS_RadList calculation of 8.1 (4)% for $P_{KXtotal}$ (see DDEP file for fully separated ^{103m}Rh decay data).

The absolute emission probabilities of both the KX-ray and 357.42-keV γ ray have been used to determine cross-section data for the production of ^{103}Pd from Rh targets (2009Ta10). Recommended decay data were adopted from the ENSDF evaluation of De Frenne and Jacobs (2001De37), and a difference of the order of 25% was observed between the activities obtained by means of these particular recommended X- and γ-ray photopeaks. The mass chain for A = 103 was re-evaluated in 2009 for ENSDF (2009De29):

$$P_{KX} = 76.9\ (14);\ \ P_\gamma(357\text{ keV}) = 0.0221\ (7)\ \rightarrow\ P_\gamma(357\text{ keV})/P_{KX}\text{ ratio of }0.000287\ (11)$$

Decay-data measurements by Berlyand *et al*. (2002Bf07) furnished emission probabilities for the K_α and K_β X-rays relative to the 357.42-keV γ ray to give a value of 0.000369 (11) for the P_γ(357 keV)/P_{KX} ratio, compared with the value of 0.000287 adopted and used previously (ENSDF 2002).

Effectively, the current evaluation of the ^{103}Pd decay scheme results in a recommended P_γ(357.42 keV) of 0.0267 (8)% and $P_{KXtotal}$ of 77.5 (4)% to produce a P_γ(357 keV)/P_{KX} ratio of 0.000345 (11), and the latter value is comparable with LWM and NRM weighted-mean averages of 0.000335 (15) and 0.000349 (8), respectively, that are based upon the measurements of 1976Ma37, 1978Ne09, 2002Bf07 and 2021Ri01.

KX-ray emission probability per 100 disintegrations and X-γ emission ratios of ^{103m}Rh, ^{103}Ru/^{103m}Rh and ^{103}Pd/^{103m}Rh decay.

Reference	P_{KX} (%)	$P_{K\alpha}/P_{K\beta}$	P_γ(357 keV)/P_{KX}	Target processing (if any) and detector systems
1967Br04 **^{103}Ru/^{103m}Rh**	7.00 (35)	–	–	Neutron irradiation of Ru metal to produce ^{103}Ru – purification two months after irradiation → fusion with KOH/KNO_3 to form perruthenate for dissolution in H_2SO_4 solution, followed by rapid RuO_4 distillation. Study of five ^{103}Ru/^{103m}Rh sources in equilibrium. measured growth of 20-keV X-ray – two NaI(Tl) crystal detectors; absolute ^{103}Ru activity – 4πβ-γ counting and NaI(Tl) γ detector.
1967VuZZ **^{103m}Rh**	7.7 (8)	–	–	Neutron irradiation of metallic Rh foils (^{103}Rh(n,n') ^{103m}Rh). $4\pi K_{ce}$–KX-ray coincidence technique, no earlier than 1.5 hours after irradiation – 4π proportional counter and thin NaI crystal detector.
1969Gr13 **^{103}Pd/^{103m}Rh**	8.4 (8)[a]	–	0.00085 (7) P_γ(39.753 keV)/P_{KX} = 0.0086 (11)	^{103}Pd extracted radiochemically from deuteron- and proton-irradiated Rh metallic plate and powder targets – difficult dissolution in hot H_2SO_4 solution, then Pd activity extracted by means of dimethyl-glyoxime-chelate in chloroform, and electroplated on to Cu foils. Also neutron-irradiation of 96%-enriched metallic ^{102}Pd target (in the form of strips deposited on Al-foil backing) to produce ^{103}Pd sources. electron spectra – double-focussing iron-yoke β spectrometer; γ and X-rays – Ge(Li) detector and NaI(Tl) crystal.
1969Le17 **^{103}Pd/^{103m}Rh** **^{103m}Rh**	– –	5.0 (2) Pd fraction; 4.7 (2) Rh fraction	– –	Proton irradiation of Rh foil to produce ^{103}Pd, which was dissolved electrolytically in HCl and diluted, prior to separation of Pd(II) in organic layer from Rh(III) in aqueous layer by addition of dithizone in chloroform. X-rays – NaI(Tl) and Ge(Li) detectors.
1973In07 **^{103}Ru/^{103m}Rh** **^{103m}Rh**	7.03 (44)	–	–	Thermal-neutron irradiation of Ru metal to produce ^{103}Ru –purification five weeks after irradiation → metal target dissolved in NaClO prior to electrodeposition on Au foil. measurement and attenuation of KX-rays and 39.753-keV γ ray – thin NaI(Tl) cleaved crystal; γ rays and γ-KX-ray coincidence – Ge(Li) detector; attenuation of Rh X-rays emitted by ^{102}Rh source; absolute detection efficiency of thick Rh source (^{102}Rh).
1974Sa15 **^{103m}Rh**	6.97 (28)	–	–	Variable-energy neutron irradiation of Rh metal (with a range of thickness) sandwiched between discs of pressed sulphur → thin ^{103m}Rh sources prepared after chemical separation from any resulting ^{103}Ru activity. X-rays and 4πce-X-ray coincidence – NaI(Tl) crystal.
1975Cz03 **^{103m}Rh**	6.76 (5)[b]	–	–	^{103m}Rh source prepared by elution from ^{103}Pd-^{103m}Rh generator. γ rays, X-rays and 4πce-X-ray coincidence counting – NaI(Tl) crystal.
1976Ma37 **^{103}Ru/^{103m}Rh** **^{103}Pd/^{103m}Rh**	80 (5)	–	**<u>0.000299 (9)</u>** P_γ(39.753keV)/P_{KX} = 0.00093	Thermal-neutron irradiation of Ru powder (enriched to 99% weight % 102) to produce ^{103}Ru, and Pd metal (enriched to 93% in mass 102) to produce ^{103}Pd → all sources purified radiochemically and deposited (^{103}Ru) or electroplated (^{103}Pd) on to suitable backing foils. 20- and 40-cm^3 Ge(Li) detectors; planar 0.5-cm^3 Ge(Li) detector for low-energy photons; 8-cm^3 Ge(Li) anti-Compton detector with NaI(Tl) annulus to give a photopeak-to-Compton ratio of 200:1 for 1332-keV of ^{60}Co.
1978Ne09 **^{103}Pd/^{103m}Rh**	–	–	**<u>0.000307 (10)</u>**[c]	Harwell: ^{103}Pd solution evaporated and deposited on to a paper filter. "phoswich" detector system – NaI(Tl) detector for X-rays; 40-cm^3 coaxial Ge(Li) detector for γ rays. Livermore: $^{103}PdCl_2$ flashed from a hot tungsten filament on to aluminised Mylar film. Si(Li) and Ge(Li) detectors for X- and γ rays.
1981Va22 **^{103m}Rh**	8.44 (9)[d]	–	–	^{103m}Rh source prepared by elution from ^{103}Pd-^{103m}Rh generator by means of anion exchange columns. activity measurements – liquid scintillation counter; KX-rays – two Si(Li) detectors.

Reference	P_{KX} (%)	$P_{K\alpha}/P_{K\beta}$	P_γ(357 keV)/P_{KX}	Target processing (if any) and detector systems
1994Sc43 **^{103}Ru/^{103m}Rh**	8.54 (11)	4.81 (10)	– P_γ(39.753 keV)/P_{KX} = 0.0083 (3)	Four sources of dried droplets of a ^{103}Ru solution were used to study ^{103}Ru-^{103m}Rh decay. activity measurements – well-type ionization chamber for 4πβ-γ coincidence counting; Si(Li) and HPGe detectors for X- and γ rays.
2002Bf07 **^{103}Pd/^{103m}Rh**	61.2 (23)	5.05 (18)	**<u>0.000369 (11)</u>**	Seven weightless ^{103}Pd sources from an OSGI standard. X-ray spectroscopy – OChG detector, γ-ray spectroscopy – 40- and 80-cm^3 Ge(Li) detectors.
2004Po24 **^{103}Pd/^{103m}Rh**	–	5.1 (4)	–	Neutron-irradiation of Pd (enriched to 99.5% weight % ^{102}Pd) for 18 days, followed by radiochemical extraction of ^{103}Pd from the irradiated target to prepare 1-ml sources of HNO_3-based solutions. Data expressed at a confidence level of 0.95 (2σ). three HPGe detectors with energy resolutions of ~ 0.6, ~ 3.0 and ~ 3.2 keV for 661.7-keV γ ray of ^{137}Cs; HPGe detector with energy resolution of ~ 0.5 keV for 24-keV K_α X-ray of Sn.
2018Ri01 **^{103m}Rh**	8.25 (17)	5.07 (17)	– P_γ(39.753 keV)/P_{KX} = 0.0096 (5)	Neutron-irradiation of both a pure compacted ^{103}Rh metallic powder pellet and $RhCl_3$ powder target, followed by post-irradiation decay of short-lived ^{104,104m}Rh. Samples processed and measured in parallel: (1) X-rays → compacted ^{103}Rh pellet, and five aqueous $RhCl_3$ sources after target dissolution in small volume of water), and (2) TDCR liquid scintillation counter (five sources after dissolution of ^{103}Rh pellet, and the five existing sources of $RhCl_3$). XK_α = 6.89 (17)%; XK_β = 1.36 (3)%; XK_{total} = 8.25 (17)%; P_γ(39.75 keV) = 0.079 (4)%. Gamma-ray impurities within the sources were also assessed and quantified by means of a large coaxial HPGe detector. absolute activity – liquid scintillation counter (triple-to-double coincidence ratio method); X-rays – low-energy planar HPGe detector.
2021Ri01 **^{103}Pd/^{103m}Rh**	71.1 (6)	4.90 (6)	**<u>0.000350 (4)</u>** P_γ(39.753keV)/P_{KX} = 0.000910 (13)	^{103}Pd supplied by NORDION in 2019 ($PdCl_3$ in dilute NH_4OH, and stabilized subsequently by addition of HCl). Six point sources prepared by means of deposition and drying on Mylar sheets sealed with a thin foil for γ-ray spectroscopy, and six sources of ~ 20-fold dilution for liquid scintillation counting; P_γ(357 keV)/P_{KX} uncertainty of ± 0.000004 adjusted to ± 0.000006 to reduce weighting from 0.6712 to 0.50 in the LWM calculations. mass activity – TDCR liquid scintillation counter, γ-ray spectroscopy – two 100-cm^3 coaxial HPGe detectors for 50 to 500 keV γ rays; planar HPGE detector for low-energy γ and X-rays; silicon drift detector (SDD) for L X-rays.
mean value	–	–	**0.000335 (15) LWM** **0.000349 (8) NRM**	χ^2/(N-1) = 13.43; $\chi^2/(N-1)_{cric}$ = 3.78 at 99% confidence χ^2/(N-1) = 4.39; $\chi^2/(N-1)_{cric}$ = 2.60 at 95% confidence

[a] Obtained by multiplying measurement of K-shell conversion-electron emission probability by 1969Gr13 of 10.4 (9) with K-shell fluorescence yield (0.807 (31), 1972Bb16).
[b] Quantified in the abstract, but not mentioned within the main text of the paper (1975Cz03).
[c] Weighted mean of three measurements coupled with an uncertainty aligned with the smallest uncertainty involved in the calculation of the average value (0.000331 (22) – Harwell, UK; 0.000316 (25) – Harwell, UK; 0.000301 (10) – Livermore, USA).
[d] Weighted mean of five measurements coupled with an uncertainty aligned with the smallest uncertainty involved in the calculation of the average value (8.20 (21), 8.40 (21), 8.47 (11), 8.54 (12), 8.42 (9)).

Measured Auger-electron intensities and intensity ratios identified with ^{103}Pd-^{103m}Rh decay.

P_{Ae}	1955Av11[a]	1969Gr13[b] (%)	2000KoZQ	2000KoZS (%)
KLL	0.27 (2)	12.3 (11)	–	–
KLX	0.10 (1)	5.2 (7)	–	–
KXY	–	0.56 (25)	–	–
$KL_1L_2(^3P_0)/(^1P_1)$ ratio	–	–	0.21 (3)	–
$KL_1L_1(^1S_0)$	–	–	–	10.4 (4)
$KL_1L_2(^1P_1)$	–	–	–	13.3 (3)
$KL_1L_2(^3P_0)$	–	–	–	2.9 (3)
$KL_1L_3(^3P_1)$	–	–	–	9.0 (4)
$KL_1L_3(^3P_2)$	–	–	–	2.0 (4)
$KL_2L_2(^1S_0)$	–	–	–	3.2 (3)
$KL_2L_3(^1D_2)$	–	–	–	43.2 (9)
$KL_3L_3(^3P_0)$	–	–	–	2.0 (4)
$KL_3L_3(^3P_2)$	–	–	–	14.0 (5)

[a] Emission probabilities expressed relative to total 37-keV L conversion-electron emission of 1.0.
[b] Emission probabilities expressed as percentage of total decay.

Further measurements of the X- and γ-ray emission probabilities are highly desirable to assist in resolving the current difficulties in the proposed decay scheme that create significant anomalies of the order of 25% in the derivation of ^{103}Pd production cross sections. This disparity is most likely to occur as a consequence of the difficulty in quantifying both the KX-ray and low-energy γ-ray emissions to the necessary precision, particularly the important but rather ill-defined P_γ(39.753 keV) – the value of this specific parameter impacts significantly on the γ-ray normalisation factor, all resulting absolute γ-ray emission probabilities, and component P_{KX} data. These relatively low-energy photon emissions need to be quantified with confidence and good accuracy in order to calculate excitation functions, and so ensure the optimum production and purity of ^{103}Pd-^{103m}Rh with confidence.

X-ray decay data for ^{103}Pd/^{103m}Rh have been measured experimentally over many years, and most recently by Riffaud *et al.* (2021Ri01). Both X-ray and Auger-electron data have been calculated on the basis of the evaluated gamma-ray data, along with atomic data from 1996Sc06, 1998ScZM, 1999ScZX and 2000Sc47 (Rh: ω_K = 0.809 (4); ϖ_L = 0.0494 (12); n_{KL} = 0.987 (4)). Both the X-ray and Auger-electron spectra for the EC decay of ^{103}Pd/^{103m}Rh have been calculated by means of the BrIccEmis code within NS-RadList, as described in 2012Le09, 2013LeZX, 2016Le19, 2020TeZY and 2023Texx in order to achieve the necessary detail and resolution of these spectral lines. A vacancy reaching the valence shell is immediately filled by an electron from the surrounding condensed-phase material to generate more atomic radiation, and this process will terminate when all such vacancies are filled below the valence shell. Transition energies within each propagation step were derived from the atomic binding energies determined by means of the relativistic Dirac-Fock approach employed in the RAINE code (2002Ba85), along with the application of a semi-empirical correction procedure that aligns these energies more fully with known spectral data (2020TeZY). Fixed transition rates were obtained from the EADL database (1991PeZY, 1993Cu08). Resulting X-ray energies and emission probabilities are listed below for ^{103}Pd, followed by the recommended Auger-electron energies and emission probabilities (both sets of energies are listed as mean energies and as a range of energies at the 95% confidence level, with additional extensions of these energy ranges in italicsfor specific of X-ray and Auger electron emissions). The number of simulated nuclear events is 10^6, and the intensity cut-off for these listings is 0.01 per 100 decays. Quoted uncertainties include direct contributions from only electron capture and internal-conversion electrons (2023Texx) – these data do not include significant uncertainties from the more complex but less well-defined atomic radiation probabilities as considered semi-quantitatively in EADL (1991PeZY). As defined by 1991PeZY, uncertainties in these theoretical X-ray emission probabilities are ~ 10% for the K and L shells and can be of the order of 30% and more for the outer shells, whereas uncertainties in the theoretical Auger-electron emission probabilities are < 15% for the K and L shells (except for Coster-Kronig and super Coster-Kronig transitions) and of the order of 30% and more for the Coster-Kronig and super Coster-Kronig transitions and the outer shells.

X-ray energies and emission probabilities of ^{103}Pd/^{103m}Rh (BrIccEmis/NS_RadList).

		Mean Energy (keV)	Energy (keV) 95% confidence range/extension	Photons per 100 decays[a]
X_{tot}	(Rh)	18.640	2.703 – 22.725	87.0 (4)
XK_{tot}	(Rh)	20.599	20.073 – 23.167/*23.173*	77.5 (4)
XKL2	(Rh)	20.073	20.073	22.36 (11)
XKL3	(Rh)	20.215	20.215	42.39 (20)
XKM	(Rh)	22.717	22.699 – 22.725	10.68 (5)
XKM2	(Rh)	22.699	22.699	3.606 (17)
XKM3	(Rh)	22.725	22.725	7.021 (33)
XKN	(Rh)	23.171	23.167 – 23.173	2.104 (10)
XKN2	(Rh)	23.167	23.167	0.7169 (34)
XKN3	(Rh)	23.173	23.173	1.383 (7)
XL_{tot}	(Rh)	2.747	2.378 – 3.094	9.24 (10)
XM_{tot}	(Rh)	0.324	0.188 – 0.553	0.2595 (23)
XN_{tot}	(Rh)	0.048	0.029 – 0.063	0.02001 (14)

[a] Quoted uncertainties include direct contributions from only electron capture and internal-conversion electrons (2023Texx) – these data do not include significant uncertainties from the more complex but less well-defined atomic radiation probabilities as considered semi-quantitatively in EADL, whereby uncertainties in the theoretical X-ray radiative rates are ~ 10% for the K and L shells, and can be of the order of 30% for the outer shells (1991PeZY).

Auger-electron energies and emission probabilities of ^{103}Pd/^{103m}Rh (BrIccEmis/NS_RadList).

		Mean Energy (keV)	Energy (keV) 95% confidence range/extension	Electrons per 100 decays[a]
Auger total	(Rh)	0.650	0.002 – 2.632	1283 (12)
Auger K_{tot}	(Rh)	17.708	16.281 – 21.922/*22.838*	18.42 (9)
Auger KLL	(Rh)	16.811	16.281 – 17.083	12.90 (6)
Auger KLX	(Rh)	19.574	19.133 – 20.146	5.043 (24)
Auger KXY	(Rh)	22.275	21.922 – 22.838	0.4760 (23)
Auger L_{tot}	(Rh)	2.027	*0.004*/0.044 – 2.768/*3.260*	195.0 (20)
Auger Coster-Kronig LLM	(Rh)	0.040	0.004 – 0.051	10.41 (+22-17)
Auger Coster-Kronig LLX	(Rh)	0.142	0.031 – 0.385	13.68 (15)
Auger LMM	(Rh)	2.236	1.842 – 2.490	143.1 (15)
Auger LMX	(Rh)	2.603	2.370 – 2.824	26.45 (28)
Auger LXY	(Rh)	2.977	2.851 – 3.260	1.339 (14)
Auger M_{tot}	(Rh)	0.198	*0.016*/0.041 – 0.369/*0.394*	514 (5)
Auger Coster-Kronig MMX	(Rh)	0.097	0.016 – 0.178	149.5 (13)
Auger MXY	(Rh)	0.239	0.140 – 0.394	364.6 (35)
Auger N_{tot}	(Rh)	0.019	0.001 – 0.034/*0.058*	555 (5)
Auger super Coster-Kronig NNN	(Rh)	0.019	0.001 – 0.034	525 (5)
Auger Coster-Kronig NNX	(Rh)	0.018	0.002 – 0.058	30.46 (21)

[a] Quoted uncertainties include direct contributions from only electron capture and internal-conversion electrons (2023Texx) – these data do not include significant uncertainties from the more complex but less well-defined atomic radiation probabilities as considered semi-quantitatively in EADL, whereby uncertainties in the theoretical Auger-electron radiative rates are < 15% for the K and L shells (except for Coster-Kronig and super Coster-Kronig transitions), and can be of the order of 30% or more for Coster-Kronig and super Coster-Kronig transitions and the outer shells (1991PeZY).

Total energy release per decay as determined from the BrIccEmis/NS_RadList studies:

Radiation	Total energy (keV per decay)	Total intensity (%)
Neutrinos	514.8 (21)	–
Gamma rays	0.157 (3)	0.1055 (33)
Conversion electrons	35.2 (+12-11)	100 (+4-3)
Auger electrons	8.32 (8)	1283 (12)
X-rays	16.21 (8)	87.1 (4)
Total	574.7 (25)	

The final X-ray and Auger-electron spectra were effectively evaluated from one million simulated nuclear decay events. Both component spectra of the Auger-electron and X-ray emissions as calculated by the BrIccEmis code for the EC decay of ^{103}Pd are shown in the following figure.

Auger-electron (upper panel) and X-ray (lower panel) spectra of ^{103}Pd EC decay:

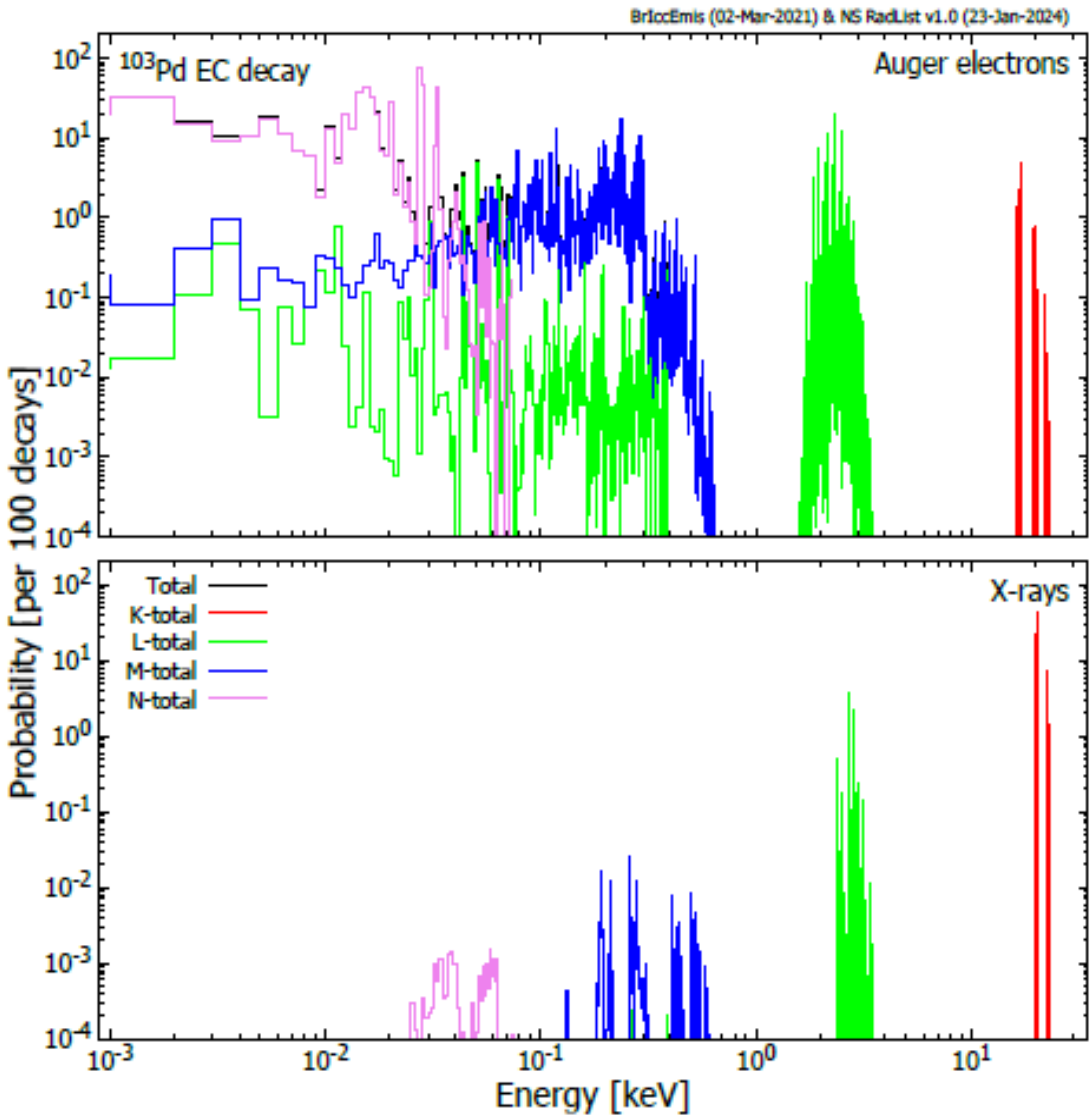

The IT decay of ^{103m}Rh has been included as part of the decay scheme of ^{103}Pd in this particular evaluation, as well as treated separately elsewhere to produce an entirely independent file. Auger-electron data have also been calculated by means of the BrIccEmis code to aid in both the generation and resolution of extensive spectral lines for confident application in microdosimetry.

Main Production Modes for ^{103}Pd

^{103}Pd:	^{102}Pd(n,γ)^{103}Pd,	^{nat}Pd(n,xn)^{103}Pd,	^{103}Rh(p,n)^{103}Pd,	^{107}Ag(p,αn)^{103}Pd,
	^{102}Pd(d,p)^{103}Pd,	^{103}Rh(d,2n)^{103}Pd,	^{107}Ag(d,α2n)^{103}Pd,	^{103}Rh(α,p3n)^{103}Pd,
	^{nat}Ag(p,2pxn)^{103}Pd,	^{nat}In(p,4pxn)^{103}Pd		

Data Consistency

^{103}Pd/^{103m}Rh

A Q_{EC}-value of 534.9 (24) keV to the metastable excited state of ^{103m}Rh has been adopted from the atomic mass evaluation 2020 of Wang *et al*. (2021Wa16), and Q_{IT}-value of 39.753 (6) keV for ^{103m}Rh IT decay to the ground state of ^{103}Rh have been adopted from NUBASE2020 as formulated by Kondev *et al.* (2021Ko07) while in the course of defining the decay scheme of ^{103}Pd. These data total to a Q_{EC}-value of 574.7 (24) keV when defined in terms of a ^{103}Pd ground-state to ^{103}Rh ground-state decay, which has been

compared with the Q-value calculated by summing the contributions of the individual emissions to the ^{103}Pd EC-decay and ^{103m}Rh IT-decay processes (i.e., EC, electron, γ, etc.):

$$\text{calculated Q-value} = \sum (E_i \times P_i) = 574.7\ (25)\ \text{keV}$$

Percentage deviation from the Q-value of Wang *et al*. is (0.0 ± 0.6)%, which supports the derivation of a consistent decay scheme with a modest variant.

References

1944Fl01 A. Flammersfeld, Kernanregung durch Schnelle Neutronen bei Rhodium und Silber, Naturwissenschaften **32** (1944) 36-37. [^{103m}Rh half-life]

1945Wi03 M.L. Wiedenbeck, The Nuclear Excitation of Krypton and Rhodium, Phys. Rev. **68** (1945) 237-239. [^{103m}Rh half-life]

1945Wi12 M.L. Wiedenbeck, The Nuclear Excitation of Rhodium, Phys. Rev. **67** (1945) 267-268. [^{103m}Rh half-life]

1947Fl03 A. Flammersfeld, O. Bruna, Die Anregungsenergie der Isomeren Zustände des Rhodiums 103 und 104, Z. Naturforsch. **2a** (1947) 241-244. [^{103m}Rh half-life]

1947Ma32 D.E. Matthews, M.L. Pool, X-ray Emission from Radioactive Ce, Pd and Ca, Phys. Rev. **72** (1947) 163-164, G8. [^{103}Pd half-life]

1948Li03 M. Lindner, I. Perlman, Neutron Deficient Isotopes of Rhodium and Palladium, Phys. Rev. **73** (1948) 1202-1203. [^{103}Pd half-life]

1950Ko10 E. Kondaiah, Disintegration of Ru^{103}, Phys. Rev. **79** (1950) 891-892. [K/(L+M) ratio (40 keV)]

1950Me26 J.Y. Mei, C.M. Huddleston, A.C.G. Mitchell, The Disintegration of Ruthenium-103 and Palladium-103, Phys. Rev. **79** (1950) 429-432. [^{103m}Rh half-life]

1952Co16 J.M. Cork, J.M. LeBlanc, F.B. Stumpf, W.H. Nestor, The Radioactive Decay of Ruthenium 103, Phys. Rev. **86** (1952) 575-576. [K/L ratios]

1953Me24 W.W. Meinke, Half-life of Pd^{109} and Neutron Activation Cross Section of Pd^{102}, Phys. Rev. **90** (1953) 410-412. [^{103}Pd half-life]

1954Ri09 L.H.Th. Rietjens, H.J. Van Den Bold, P.M. Endt, Continuous and Discrete Gamma-radiation in the Decay of ^{103}Pd, Physica **20** (1954) 107-114. [^{103}Pd half-life, E_γ, P_γ]

1955Av11 P. Avignon, A. Michalowicz, R. Bouchez, Étude de la Désintégration du ^{103}Pd, J. Phys. Radium **16** (1955) 404-410. [E_γ, P_γ, α_K, α_L, K/L ratio]

1955Dr43 G.M. Drabkin, V.I. Orlov, L.I. Rusinov, Investigation of the Nuclear Isomerism of Zn^{69}, Se^{79}, Se^{81}, Rh^{103} and Ba^{137}, Izvest. Akad. Nauk SSSR, Ser. Fiz., Columbia Tech. Transl. **19** (1956) 294-304. [α_K, K/L and L/M ratios]

1955Mc51 F.K. McGowan, P.H. Stelson, Angular Distribution of Gamma Rays from Coulomb Excitation, Phys. Rev. **99** (1955) 127-134. [δ (295 keV)]

1955Sa16 B. Saraf, Energy Levels of Rh^{103} from the Decay of Pd^{103} and Ru^{103}, Phys. Rev. **97** (1955) 715-720. [E_γ, P_γ]

1957Jo19 G.A. Jones, W.R. Phillips, Electrical Octupole Coulomb Excitation in Rhodium, Proc. Royal Soc. (London) **239A** (1957) 487-493. [^{103m}Rh half-life]

1958Mc02 F.K. McGowan, P.H. Stelson, Yields, Angular Distributions, and Polarization of Gamma Rays from Coulomb Excitation, Phys. Rev. **109** (1958) 901-916. [δ (295 keV)]

1967Br04 A.M. Bresesti, M. Bresesti, H. Neumann, Measurement of K X-ray Emission in the Decay of ^{103m}Rh, J. Inorg. Nucl. Chem. **29** (1967) 15-20.
[^{103}Ru β^- decay: P_{KX}, K/(L+M+N) ratio of 39.75-keV gamma transition]

1967VuZZ A. Vuorinen, Calibration of ^{103m}Rh by the Coincidence Method, pp. 257-263, Proc. Symp. Standardization of Radionuclides, IAEA, Vienna, Austria (1967).
[^{103m}Rh half-life, K/(K + L + M) ratio, P_{KX} of 39.75-keV gamma transition]

1968Ha52 R.S. Hager, E.C. Seltzer, Internal Conversion Tables, Part 1: K-, L-, M-shell Conversion Coefficients for Z = 30 to Z = 103, Nucl. Data **A4** (1968) 1-235. [Theoretical ICC]

1968Ma08 J.C. Manthuruthil, H.J. Hennecke, C.R. Cothern, Internal-Conversion-Electron Study of the Decay of Ru^{103}, Phys. Rev. **165** (1968) 1363-1370. [ICC, multipolarities, mixing ratios]

1968Pa24 J.A. Panontin, N.T. Porile, A.A. Caretto, Jr., Nuclear Reactions of Silver and Indium with 200- and 400-MeV Protons, Phys. Rev. **165** (1968) 1273-1281. [^{103}Pd half-life]

1969Gr13 Y. Grunditz, S. Antman, H. Pettersson, M. Saraceno, Studies in the Decay of ^{103}Pd, Nucl. Phys. **A133** (1969) 369-384.
[^{103}Pd half-life, E_γ, P_γ, α_K, subshell ratios, P_{KX} and P(357 keV)/P_{KX} ratio of ^{103}Pd-^{103m}Rh]

1969KoZW Y. Kobayashi, Half-lives of Rhodium-106, -105 and -103m, JAERI report JAERI-1178 (1969) 21-22. [^{103m}Rh half-life]

1969Le17 M.A. Lepri, W.S. Lyon, Decay of ^{103}Pd–^{103m}Rh, Int. J. Appl. Radiat. Isot. **20** (1969) 297-298.
[K_α/K_β ^{103}Pd-^{103}Rh, 39.75-keV α_K]

1969Ra18 D.E. Raeside, J.J. Reidy, M.L. Wiedenbeck, The Levels of ^{103}Rh Populated in the Decay of ^{103}Ru, Nucl. Phys. **A134** (1969) 347-352. [E_γ, α_K]

1969Zo02 W.H. Zoller, E.S. Macias, M.B. Perkal, W.B. Walters, Decay of 40 d ^{103}Ru and 17 d ^{103}Pd to Levels of ^{103}Rh, Nucl. Phys. **A130** (1969) 293-304. [E_γ, P_γ, α_K(497 keV), γ-γ]

1970NiZV E.B. Nieschmidt, D.A. Pearson, Nuclear Levels of ^{103}Rh, IN-1317 (1970) 122-126.
[E_γ, P_γ, α_K, L subshell ratios]

1970Pe04 H. Pettersson, S. Antman, Y. Grunditz, Studies in the Decay of ^{103}Ru, Z. Phys. **233** (1970) 260-274; Erratum, Z. Phys. **235** (1970) 485. [E_γ, L_1/L_2, L_1/L_3, L_2/L_3 ratios, α_K]

1970RoZS W.M. Roney, H.W. Kugel, G.M. Heestand, R.R. Borchers, R. Kalish, Magnetic Moments of Core Excited States of Odd Nuclei Near A = 100, pp. 419-423 in Proc. Int. Conf. Nuclear Reactions Induced by Heavy Ions, 15-18 July 1969, Heidelberg, Germany, Editors: R. Bock, W.R. Hering, North-Holland Pub. Corp., Amsterdam (1970). [δ (295 keV)]

1971Av03 F.T. Avignone III, G.D. Frey, Internal-conversion and γ−γ Directional-correlation Studies in the Decay of ^{103}Ru, Phys. Rev. **C4** (1971) 912-918. [α_K, K/(L+M+ ….) ratio, multipolarity]

1972Bb16 W. Bambynek, B. Crasemann, R.W. Fink, H.-U. Freund, H. Mark, C.D. Swift, R.E. Price, P. Venugopala Rao, X-Ray Fluorescence Yields, Auger, and Coster-Kronig Transition Probabilities, Rev. Mod. Phys. **44** (1972) 716-813; Erratum, Rev. Mod. Phys. **46** (1974) 853. [K-shell fluorescence yield]

1972Br02 D.S. Brenner, M.L. Perlman, Subshell Conversion-line Intensity Ratios for Some Pure Transitions, Nucl. Phys. **A181** (1972) 207-216. [39.75-keV L_1/L_3, L_2/L_3 ratios]

1972Ja01 H.C. Jain, S.K. Bhattacherjee, C.V.K. Baba, Half-lives of 9/2$^+$ Levels in Some Odd-mass Rh and Ag Nuclei, Nucl. Phys. **A178** (1972) 437-448. [93-keV level half-life of ^{103}Rh]

1972Pa10 A. Pazsit, J. Csikai, Cross Sections of the Reactions In^{113}(n,n')In^{113m} and Rh^{103}(n,n')Rh^{103m}, Sov. J. Nucl. Phys. **35** (1972) 232-233. [^{103m}Rh half-life, α_K(39.75 keV)]

1972Sa03 R.O. Sayer, J.K. Temperley, D. Eccleshell, Negative Parity Levels in ^{103}Rh via Coulomb Excitation, Nucl. Phys. **A179** (1972) 122-140. [δ (295 keV)]

1973Ba32 Chr. Bargholtz, J. Becker, L. Eriksson, L. Gidefeldt, L. Holmberg, V. Stefánsson, Gamma-gamma Directional Correlations in ^{103}Rh, Phys. Scr. **8** (1973) 90-94. [93-keV level half-life of ^{103}Rh]

1973Gu06 E. Günther, K. Knauf, K.F. Walz, The Half-life of ^{103m}Rh, Int. J. Appl. Radiat. Isot. **24** (1973) 87-89. [^{103m}Rh half-life]

1973In07 H. Ing, W.G. Cross, Absolute Counting of K X-rays from ^{103m}Rh in Thick Foils, Int. J. Appl. Radiat. Isot. **24** (1973) 437-450. [^{103}Ru β^- decay: P_{KX} of ^{103}Ru-^{103m}Rh]

1974CzZY K.H. Czock, N. Haselberger, F. Reichel, The Disintegration of ^{103m}Rh, IAEA report IAEA/RL/26 (1974). [α_{total}, α_K, K/(L + M + …..) ratio]

1974Sa15 D.C. Santry, J.P. Butler, Cross Section Measurements for the ^{103}Rh(n,n') ^{103m}Rh Reaction from 0.122 to 14.74 MeV, Can. J. Phys. **52** (1974) 1421-1428. [^{103m}Rh half-life, P_{KX} of ^{103m}Rh]

1975Cz03 K.H. Czock, N. Haselberger, F. Reichel, The Disintegration of ^{103m}Rh, Int. J. Appl. Radiat. Isot. **26** (1975) 417-421. [α_{total}, α_K, P_{KX} of ^{103m}Rh]

1975Cz05 K.H. Czock, N. Haselberger, F. Reichel, S. Popa, Determination of the Half-life of ^{103}Pd, Int. J. Appl. Radiat. Isot. **26** (1975) 782-784. [^{103}Pd half-life]

1975Ma32 B. Martin, D. Merkert, J.L. Campbell, Intensity Ratios of L, M, N, O Subshell Conversion Electrons in M3 and E4 Transitions, Z. Phys. **A274** (1975) 15-21. [39.75-keV L_1/L_2, L_1/L_3, L_2/L_3, M, N, O ratios]

1976Ma37 E.S. Macias, M.E. Phelps, D.G. Sarantites, R.A. Meyer, Decay of 39-day ^{103}Ru and 17-day ^{103}Pd to the Levels of ^{103}Rh, Phys. Rev. **C14** (1976) 639-644. [E_γ, P_γ, α_K, α_L, P_{KX} and P(357 keV)/P_{KX} ratio of ^{103}Pd-^{103m}Rh]

1977Kr13 K.S. Krane, E2, M1 Multipole Mixing Ratios in Odd-mass Nuclei 59 ≤ A ≤ 149, At. Data Nucl. Data Tables **19** (1977) 363-416. [δ]

1977La19 F.P. Larkins, Semiempirical Auger-electron Energies for Elements 10 ≤ Z ≤ 100, At. Data Nucl. Data Tables **20** (1977) 311-387. [Auger-electron energies]

1978La21 F. Lagoutine, J. Legrand, C. Bac, Périodes de Quelques Radionucléides, Int. J. Appl. Radiat. Isot. **29** (1978) 269-272. [^{103m}Rh half-life]

1978Ne09 D. Newton, A.E.R. Toureau, A.L. Anderson, R.A. Meyer, Relative High-energy Gamma- and X-ray Emissions Following the Decay of ^{103}Pd, Int. J. Appl. Radiat. Isot. **29** (1978) 188-189. [E_γ, P_γ, P(357 keV)/P_{KX} ratio of ^{103}Pd-^{103m}Rh]

1979VaZE R. Vaninbroukx, G. Grosse, W. Zehner, Studies of the Decay of ^{103m}Rh, NEA report NEANDC(E)-202U, Vol. III (1979) 28-30. [P_γ, P_{KX}, α_{total}, α_K of ^{103m}Rh]

1981Ha11 E. Hagn, J. Wese, G. Eska, Nuclear Orientation Study of ^{97,103,105}Ru in Fe, Z. Phys. – Atoms and Nuclei **A299** (1981) 353-358. [497.1-keV δ]

1981Mu18 D.W. Murray, A.L. Allsop, N.J. Stone, The Magnetic Moment of ^{103}Ru, Hyperfine Interactions **11** (1981) 127-139. [497.1-keV δ]

1981Va11 R. Vaninbroukx, G. Grosse, W. Zehner, New Determinations of the Half-lives of ^{57}Co, ^{103}Ru, ^{103m}Rh, ^{103}Pd and ^{109}Cd, Int. J. Appl. Radiat. Isot. **32** (1981) 589-591. [^{103}Pd and ^{103m}Rh half-lives]

1981Va22 R. Vaninbroukx, W. Zehner, Determination of the K X-ray Emission Probability in the Decay of ^{103m}Rh, Int. J. Appl. Radiat. Isot. **32** (1981) 850. [^{103m}Rh P_{KX}]

1983Kr01 K.S. Krane, Nuclear orientation of ^{103}Ru: Re-analysis, Phys. Rev. **C27** (1983) 411-412. [497.1-keV δ]

1991PeZY S.T. Perkins, D.E. Cullen, M.H. Chen, J.H. Hubbell, J. Rathkopf, J. Scofield, Tables and Graphs of Atomic Subshell and Relaxation Data Derived from the LLNL Evaluated Atomic Data Library (EADL), Z = 1–100, Lawrence Livermore National Laboratory report UCRL-50400, **30** (1991). [atomic database]

1993Cu08 D.E. Cullen, S.T. Perkins, S.M. Seltzer, Photon and Electron Databases and Their Use in Radiation Transport Calculations, Appl. Radiat. Isot. **44** (1993) 1343-1347. [atomic database]

1994Sc43 U. Schötzig, Photon Emission Probabilities in the Decay of ^{103}Ru/^{103m}Rh, Appl. Radiat. Isot. **45** (1994) 641-644. [^{103m}Rh P_{KX}]

1995ScZY E. Schönfeld, Tables for the Calculation of Electron Capture Probabilities, PTB Report PTB-6.33-95-2, 1995. [P_K, P_L, P_M, P_N, P_O]

1996Sc06 E. Schönfeld, H. Janβen, Evaluation of Atomic Shell Data, Nucl. Instrum. Methods Phys. Res. **A369** (1996) 527-533. [ω_K, ϖ_L, K_β/K_α, $K_{\alpha2}/K_{\alpha1}$, KLX/KLL, KXY/KLL]

1998Sc28 E. Schönfeld, Calculation of Fractional Electron Capture Probabilities, Appl. Radiat. Isot. **49** (1998) 1353-1357. [P_K, P_L, P_M, P_N, P_O]

1998ScZM E. Schönfeld, G. Rodloff, Tables of the Energies of K-Auger Electrons for Elements with Atomic Numbers in the Range from Z = 11 to Z = 100, PTB Report PTB-6.11-98-1, October 1998. [Auger electrons]

1999Sa78 M. Sainath, K. Venkataramaniah, Measurement of α_K, α_L, α_M of the Hindered E3 Transition in ^{103}Rh, Indian J. Pure Appl. Phys. **37** (1999) 87-91. [39.75-keV α_K, α_L, α_M]

1999ScZX E. Schönfeld, G. Rodloff, Energies and Relative Emission Probabilities of K X-rays for Elements with Atomic Numbers in the Range from Z = 5 to Z = 100, PTB Report PTB-6.11-1999-1, February 1999. [X_K]

2000KoZQ A. Kovalík, E.A. Yakushev, D.V. Filosofov, A.F. Novgorodov, V.M. Gorozhankin, I. Štekl, P. Petev, M.A. Mahmoud, The Predicted Strong Influence of the Relativistic Effects on the $KL_1L_2(^3P_0)$ Auger Transition Rate Proved for Z = 32, 45, 59 and 61, Program and Thesis, Proc. 50th Ann. Conf. Nucl. Spectrosc. Struct. At. Nuclei, St. Petersburg, Russia (2000) 178. [^{103}Rh KL_1L_2 Auger spectrum]

2000KoZS A. Kovalík, A.F. Novgorodov, E.A. Yakushev, V.M. Gorozhankin, P. Petev, M.A. Mahmoud, The KLL Auger Spectrum of $^{103}_{45}Rh$ from the EC Decay of $^{103}_{46}Pd$, Program and Thesis, Proc. 50th Ann. Conf. Nucl. Spectrosc. Struct. At. Nuclei, St. Petersburg, Russia (2000) 176. [^{103}Rh KLL Auger spectrum]

2000KoZT A. Kovalík, E.A. Yakushev, D.V. Filosofov, V.M. Gorozhankin, V.G. Kalinnikov, Energies of the 39.7 keV E3 Transition in ^{103}Rh, the 25.6 keV E1 Transition in ^{161}Dy, the 74.6 keV and 76.2 keV M1 Transitions in ^{161}Ho, and 67.2 keV E3 and 71.9 keV M1 + E2 Transitions in ^{158}Ho, Program and Thesis, Proc. 50th Ann. Conf. Nucl. Spectrosc. Struct. At. Nuclei, St. Petersburg, Russia (2000) 175. [39.7537(21)-keV γ-ray energy ^{103m}Rh]

2000Sc47 E. Schönfeld, H. Janβen, Calculation of Emission Probabilities of X-rays and Auger Electrons Emitted in Radioactive Disintegration Processes, Appl. Radiat. Isot. **52** (2000) 595-600. [P_X, P_{Ae}]

2001De37 D. De Frenne, E. Jacobs, Nuclear Data Sheets for A = 103, Nucl. Data Sheets **93** (2001) 447-598. [Nuclear levels]

2002Ba85 I.M. Band, M.B. Trzhaskovskaya, C.W. Nestor, Jr., P.O. Tikkanen, S. Raman, Dirac–Fock Internal Conversion Coefficients, At. Data Nucl. Data Tables **81** (2002) 1-334. [Theoretical ICC]

2002Bf07 T.P. Berlyand, E.I. Grigor'ev, V.P. Orlov, Measurement of the Relative Intensity of ^{103}Pd Photon Radiation, Measurement Techniques **45** (2002) 974-977. [^{103}Pd EC decay: P_γ, P_X, K_α/K_β, P(357 keV)/P_{KX} ratio of ^{103}Pd-^{103m}Rh]

2002Ra45 S. Raman, C.W. Nestor, Jr., A. Ichihara, M.B. Trzhaskovskaya, How Good are the Internal Conversion Coefficients Now? Phys. Rev. **C66** (2002) 044312, 1-23. [Theoretical ICC]

2004Po24 Yu.S. Popov, L.V. Zakharova, V.N. Kupriyanov, O.I. Andreev, A.N. Pakhomov, F.Z. Vakhetov, Half-life and Photon Intensities of ^{103}Pd, Radiochemistry **46** (2004) 209-210. [^{103}Pd half-life, P_γ, P_X, K_α/K_β]

2008Ki07 T. Kibédi, T.W. Burrows, M.B. Trzhaskovskaya, P.M. Davidson, C.W. Nestor, Jr., Evaluation of Theoretical Conversion Coefficients using BrIcc, Nucl. Instrum. Methods Phys. Res. **A589** (2008) 202-229. [Theoretical ICC]

2009De29 D. De Frenne, Nuclear Data Sheets for A = 103, Nucl. Data Sheets **110** (2009) 2081-2256. [Nuclear levels]

2009Ta10 F. Tárkányi, A. Hermanne, B. Király, S. Takács, F. Ditrói, J. Csikai, A. Fenyvesi, M.S. Uddin, M. Hagiwara, M. Baba, T. Ido, Yu.N. Shubin, A.V. Ignatyuk, New Cross Sections for Production of ^{103}Pd – Review of Charged-particle Production Routes, Appl. Radiat. Isot. **67** (2009) 1574-1581. [Discrepancies in P_γ and P_{KX}]

2010Kr05 K.S. Krane, Neutron Capture by Ru: Neutron Cross Sections of ^{96,102,104}Ru and γ-ray Spectroscopy in the Decays of ^{97,103,105}Ru, Phys. Rev. **C81** (2010) 044310, 1-10. [E_γ, ^{103}Rh nuclear level energies]

2012Le09 B.Q. Lee, T. Kibédi, A.E. Stuchbery, K.A. Robertson, Atomic Radiations in the Decay of Medical Radioisotopes – A Physics Perspective, Comput. Math. Methods Med. Article ID 651475 (2012) 1-14, doi:10.1155/2012/651475. [Atomic radiation]

2013LeZX B.Q. Lee, T. Kibédi, A.E. Stuchbery, K.A. Robertson, F.G. Kondev, A Model to Realize the Potential of Auger Electrons for Radiotherapy, Proc. Heavy Ion Accelerator Symposium (HIAS2013), 8-12 April 2013, Canberra, Australia, EPJ Web of Conferences, **63** (2013) 01002, 1-5, editors: C. Simenel, M. Evers, T. Kibédi, D. Huy Luong, M. Reed, M. Srncik, A. Wallner; doi.org/10.1051/epjconf/20136301002. [Auger electrons]

2015Mo10 X. Mougeot, Reliability of Usual Assumptions in the Calculation of β and ν Spectra, Phys. Rev. **C91** (2015) 055504, 1-12; Erratum, Phys. Rev. **C92** (2015) 059902, 1. [β decay (BetaShape code)]

2016Le19 B.Q. Lee, Hooshang Nikjoo, J. Ekman, P. Jönsson, A.E. Stuchbery, T. Kibédi, A Stochastic Cascade Model for Auger-electron Emitting Radionuclides, Int. J. Radiat. Biol. **92** (2016) 641-653; doi: 10.3109/09553002.2016.1153810. [Atomic radiation]

2018Ni14 N. Nica, J.C. Hardy, V.E. Iacob, V. Horvat, H.I. Park, T.A. Werke, K.J. Glennon, C.M. Folden III, V.I. Sabla, J.B. Bryant, X.K. James, M.B. Trzhaskovskaya, Precise Measurement of α_K and α_T for the 39.8-keV E3 transition in ^{103}Rh: Test of Internal-conversion Theory, Phys. Rev. **C98** (2018) 054321, 1-11. [α_K, α_T, δ (39.75-keV γ-ray transition)]

2018Ri01 J. Riffaud, P. Cassette, D. Lacour, V. Lourenço, I. Tartès, M.A. Kellett, M. Corbel, M.-C. Lépy, C. Domergue, C. Destouches, H. Carcreff, O. Vigneau, Measurement of Absolute K X-ray Emission Intensities in the Decay of ^{103m}Rh, Appl. Radiat. Isot. **134** (2018) 399-405. [^{103m}Rh IT decay: absolute P_{KX}, absolute P_γ]

2019Mo35 X. Mougeot, Towards High-precision Calculation of Electron Capture Decays, Appl. Radiat. Isot. **154** (2019) 108884, 1-8. [EC/β^+ decay (BetaShape code)]

2020TeZY B.P.E. Tee, T. Kibédi, B.Q. Lee, M. Vos, R. du Rietz, A.E. Stuchbery, Development of a New Database for Auger-electron and X-ray Spectra, Proc. Heavy Ion Accelerator Symposium (HIAS2019), 9-13 September 2019, Canberra, Australia, EPJ Web of Conferences, **232** (2020) 01006, 1-4, editors: A.J. Mitchell, S. Pavetich, D. Koll; doi.org/10.1051/epjconf/202023201006. [Atomic radiation]

2021Ko07 F.G. Kondev, Meng Wang, W.J. Huang, S. Naimi, G. Audi, The NUBASE2020 Evaluation of Nuclear Physics Properties, Chin. Phys. **C45** (2021) 030001, 1-180; doi: 10.1088/1674-1137/abddae [Q_{IT}(^{103m}Rh)]

2021Ri01 J. Riffaud, M.-C. Lépy, P. Cassette, M. Corbel, M.A. Kellett, V. Lourenço, Measurement of the Absolute Gamma-ray Emission Intensities from the Decay of ^{103}Pd, Appl. Radiat. Isot. **167** (2021) 109298, 1-9. [^{103}Pd half-life, absolute P_{KX}, relative P_{LX}, absolute P_γ]

2021Wa16 Meng Wang, W.J. Huang, F.G. Kondev, G. Audi, S. Naimi, The AME2020 Atomic Mass Evaluation (II): Tables, Graphs and References, Chin. Phys. **C45** (2021) 030003, 1-512; doi: 10.1088/1674-1137/abddaf [Q-values]

2023Mo21 X. Mougeot, Atomic Exchange Correction in Forbidden Unique Beta Transitions, Appl. Radiat. Isot. **201** (2023) 111018, 1-6. [β decay (BetaShape code)]

2023Texx B.P.E. Tee, T. Kibédi, B.Q. Lee, A.E. Stuchbery, BrIccEmisDB Database and Computational Tool to Evaluate Atomic Relaxation Radiations, in preparation for submission to At. Data Nucl. Data Tables (2023-2024). [Atomic radiation]

90 references and three errata – 93 items

ENSDF Analysis Programs:
GTOL, version 7.2h, 24 May 2013
GABS, version 12, 20 June 2021
BrIcc, version 2.3b, 16 December 2014
BrIccEmis, 2 March 2021
NS_RadList, version 1.0, 7 December 2023
BrIccMixing, version 2.3d, 28 September 2019

ENSDF Utility Programs:
Avetools, version 3.0, 11 December 2014
V.AveLib, version 06-22, 19 March 2024

FMTCHK, version 10.4d, 7 September 2022

LNHB Analysis Program
BetaShape, version 2.3.1, December 2023

The above codes have undergone and will continue to undergo various forms of modification and improvement, which will be reflected in changes to the version number and date of issue into the public domain. Assistance from Xavier Mougeot (LNHB, CEA Saclay, France – BetaShape) and Tibor Kibédi (ANU, Australia – particularly BrIccEmis) concerning improved operational features of some of the above codes is gratefully acknowledged by ALN.